Supported by

NONLINEAR CONVEX ANALYSIS AND OPTIMIZATION

An International Journal on Numerical, Computation and Applications

Volume 2 No. 1, January-June 2023

Published by

Center of Excellence

https://tacscoe.wordpress.com

https://ncao.design.blog

Aims & Scopes

The journal **Nonlinear Convex Analysis and Optimization (NCAO)**: An International Journal on Numerical, Computation and Applications, published by the Theoretical and Computational Science Center (TaCS Center) aims to publish original research papers and survey articles of high quality in mathematics areas of computational and application aspects of nonlinear analysis, convex analysis, fixed point theory, numerical optimization, optimization techniques and their applications to science and engineering, and related topics. It is planned to publish only high-quality papers consisting of material not published elsewhere. It will also occasionally publish proceedings of conferences (co)-organized by the TaCS-CoE and NCAO-Research Center, KMUTT.

Journal Information

NCAO is a peer-reviewed, open-access international journal, that devotes to the publication of original articles of current interest in every theoretical, fixed point theory, numerical optimization, and optimization technique and their applications to science and engineering. All manuscripts are refereed under the same standards as those used by the finest-quality printed mathematical journals. Accepted papers will be published online in their final form as an NCAO formatted PDF. and will be published in two issues annually in June and December.

Articles

Nonlinear Convex Analysis and Optimization
Vol. 2, No. 1, 2023, pp. 1–30
https://ncao.design.blog

An Approximation Technique for General Split Feasibility Problems Based on Projection onto the Intersection of Half-spaces

Guash Haile Taddele [a,b,1,*], Songpon Sriwongsa [a,b,2]

[a] Fixed Point Research Laboratory, Fixed Point Theory and Applications Research Group, Center of Excellence in Theoretical and Computational Science (TaCS-CoE), Faculty of Science, King Mongkut's University of Technology Thonburi (KMUTT), 126 Pracha Uthit Rd., Bang Mod, Thung Khru, Bangkok 10140, Thailand
[b] Department of Mathematics, Faculty of Science, King Mongkut's University of Technology Thonburi (KMUTT), 126 Pracha Uthit Rd., Bang Mod, Thung Khru, Bangkok 10140, Thailand
[1] guashhaile79@gmail.com; [2] songpon.sri@kmutt.ac.th
[*] Corresponding Author

ABSTRACT

This paper presents a novel relaxed CQ algorithm for solving the multiple-sets split feasibility problem with multiple output sets (MSSFPMOS) in infinite-dimensional real Hilbert spaces. The proposed method replaces the projection to half-space with the projection to the intersection of two half-spaces, resulting in accelerated convergence by utilizing previous half-spaces. The present study introduces a novel algorithm that dynamically determines the stepsize, without any a priori knowledge of the operator norm required. Furthermore, the algorithm is proven to exhibit strong convergence to the minimum-norm solution of the MSSFPMOS. Finally, a number of numerical experiments have been conducted to showcase the impressive performance of the proposed algorithm.

Article History
Received 5 Jan 2023
Accepted 23 March 2023
Keywords:
Split feasibility problem;
Self-adaptive technique;
Half-space relaxation;
Strong convergence
MSC
47H09; 47H10; 65K05; 90C25; 47J25; 97M40

1. Introduction

Let H_1 and H_2 be two real Hilbert spaces. Let $F : H_1 \to H_2$ be a bounded linear operator and $F^* : H_2 \to H_1$ be its adjoint. The split feasibility problem (SFP, for short) is to find a point

$$u^* \in C \text{ such that } Fu^* \in Q, \tag{1.1}$$

where C and Q are non-empty, closed, and convex subsets of H_1 and H_2, respectively.

Due to it's practical application, the SFP has received a great attention by many researchers, and several generalizations of it have been studied by many authors, see, for in-

Please cite this article as: G.H. Taddele and S. Sriwongsa, An Approximation Technique for General Split Feasibility Problems Based on Projection onto the Intersection of Half-spaces, Nonlinear Convex Anal. & Optim., Vol. 2 No. 1, 1–30. https://doi.org/10.58715/ncao.2023.2.1

stance, the multiple-sets split feasibility problem (MSSFP) [7], the split feasibility problem with multiple output sets (SFPMOS)[17], the split variational inequality problem (SVIP) [5].

Let H_1 and H_2 be two real Hilbert spaces. Let $F : H_1 \to H_2$ be a bounded linear operator and $F^* : H_2 \to H_1$ its adjoint. The multiple-sets split feasibility problem (MSSFP, for short) consists of finding a point $u^* \in H_1$ such that

$$u^* \in \bigcap_{i=1}^{n} C_i \text{ such that } Fu^* \in \bigcap_{j=1}^{m} Q_j,$$

where $C_1, \dots, C_n$ and $Q_1, \dots, Q_m$ are non-empty, closed, and convex subsets of H_1 and H_2, respectively and $n \geq 1$ and $m \geq 1$ are given integers.

The MSSFP, a general way to characterize various inverse problems arising in many real-world application problems, such as medical image reconstruction and intensity-modulated radiation therapy is to find a point in the intersection of a finite family of closed convex sets in one space such that its image under a linear transformation belongs to the intersection of another finite family of closed convex sets in the image space.

In the present study, we address the following problem in infinite-dimensional real Hilbert spaces.

Let H, H_j, $j = 1, 2, \dots, m$, be real Hilbert spaces and let $F_j : H \to H_j$, $j = 1, 2, \dots, m$, be bounded linear operators. The multiple-sets split feasibility problem with multiple output sets (MSSFPMOS, for short) is to find an element u^* such that

$$u^* \in \Omega := \left(\cap_{i=1}^{n} C_i \right) \cap \left(\cap_{j=1}^{m} F_j^{-1}\left(Q_j\right) \right) \neq \emptyset \tag{1.2}$$

where C_i, $i = 1, 2, \dots, n$, and Q_j, $j = 1, 2, \dots, m$, are non-empty, closed, and convex subsets of H and H_j, $j = 1, 2, \dots, m$, respectively, $n, m \geq 1$ are given integers. That is, $u^* \in C_i$ for each $i = 1, 2, \dots, n$, and $F_j u^* \in Q_j$ for each $j = 1, 2, \dots, m$.

When considering the specific scenario where $n = m = 1$, the MSSFPMOS (1.2) simplifies to the more focused SFP (1.1) [2, 3, 6].

The SFP was initially introduced by Censor and Elfving [6] as a mathematical framework for addressing inverse problems in finite-dimensional Hilbert spaces. This problem formulation has found applications in various areas, including phase retrievals and medical image reconstruction, enabling the development of effective algorithms and techniques in these fields. The SFP has also attracted significant attention, leading to the development of various iterative methods for its solution. Several references [15, 2, 8, 16, 19, 21, 22, 23, 24, 25, 26, 30] and others provide insights into these iterative approaches. However, the initial algorithm proposed by Censor and Elfving [6], which relied on computing the inverse of F at each iteration, did not gain much popularity.

A more widely adopted algorithm for solving SFP is the CQ algorithm introduced by Byrne [2]:

$$u_{t+1} = P_C(u_t - \lambda F^*(I - P_Q)Fu_t), \tag{1.3}$$

where P_C and P_Q are the metric projections onto C and Q, respectively, F^* is the adjoint of F, and the stepsize $\lambda \in \left(0,\ 2\|F\|^{-2}\right)$. Xu [23] proved the weak convergence of (1.3) in the framework of infinite-dimensional Hilbert space. To acquire strong convergence, Wang and Xu [20] presented an alternative method:

$$u_{t+1} = P_C\big((1 - \sigma_t)(u_t - \lambda F^*(I - P_Q)Fu_t)\big), \tag{1.4}$$

where $\lambda \in \left(0,\ 2\|F\|^{-2}\right)$ and $\{\sigma_t\} \subset (0,1)$ such that $\lim_{t\to\infty} \sigma_t = 0$; $\sum_{t=0}^{\infty} |\sigma_{t+1} - \sigma_t| < \infty$. They proved that the sequence $\{u_t\}$ generated by (1.4) converges strongly to the minimum-norm solution of the SFP (1.1). Later, Yu et al. [27] proved that $\{u_t\}$ generated by (1.4) is strongly convergent without the assumption $\sum_{t=0}^{\infty} |\sigma_{t+1} - \sigma_t| < \infty$.

The CQ algorithm, classified as a gradient-projection method (GPM) in convex minimization, gained recognition due to its ability to avoid the computation of the inverse of F. However, implementing this algorithm requires prior knowledge of the operator norm $\|F\|$, which can be challenging to estimate accurately due to its global invariance. Additionally, computing a projection onto a closed convex subset is generally a nontrivial task.

To overcome these challenges, Fukushima [10] proposed a method to compute the projection onto a level set of a convex function by iteratively projecting onto half-spaces that contain the original level set. This idea was extended by Yang [24] and Lopez et al. [14] to solve SFPs in finite- and infinite-dimensional Hilbert spaces, respectively. Their research focused on SFPs where the sets C and Q are represented as sublevel sets of convex functions with bounded subdifferential operators. To be specific, the sets C and Q are defined by

$$C = \{u \in H_1 : c(u) \leq 0\} \quad \text{and} \quad Q = \{v \in H_2 : q(v) \leq 0\}, \tag{1.5}$$

where $c : H_1 \to \mathbb{R}$ and $q : H_2 \to \mathbb{R}$ are convex and differentiable functions. Given the iterative point u_t, Yang [24] constructed the super sets (half-spaces) C_t and Q_t of the original set C and Q, respectively. The half-spaces C_t and Q_t are defined by

$$C_t = \{u \in H_1 : c(u_t) + \langle \xi_t,\ u - u_t \rangle \leq 0\}, \quad \text{where } \xi_t \in \partial c(u_t), \tag{1.6}$$

$$Q_t = \{v \in H_2 : q(Fu_t) + \langle \eta_t,\ v - Fu_t \rangle \leq 0\}, \quad \text{where } \eta_t \in \partial q(Fu_t). \tag{1.7}$$

Yang [24] introduced a relaxed CQ algorithm of the form:

$$u_{t+1} = P_{C_t}\Big(u_t - \lambda F^*(I - P_{Q_t})Fu_t\Big), \tag{1.8}$$

where $\lambda \in \left(0,\ 2\|F\|^{-2}\right)$ and a weak convergence of it is proved.

However, it should be noted that the stepsize λ in equation (1.8) is dependent on the operator norm $\|F\|$ or its estimation, which is typically a complex calculation. To circumvent this issue, numerous self-adaptive stepsizes have been developed. Specifically, López et al. [14] introduced a relaxed version of the CQ algorithm based on Yang's relaxed CQ algorithm for solving the SFP, where closed convex subsets C and Q are considered as level sets of convex functions. They proposed an adaptive approach to determine the stepsize sequence, addressing a limitation in the original relaxed CQ algorithm proposed by Yang [24]. In the adjusted algorithm proposed by López et al. [14], the parameter λ was substituted with a dynamic stepsize sequence $\{\tau_t\}$ that was ingeniously defined as follows:

$$\tau_t = \frac{\rho_t \|(I - P_{Q_t})Fu_t\|^2}{\|F^*(I - P_{Q_t})Fu_t\|^2}, \tag{1.9}$$

where $\rho_t \subset (0,2)$, $\forall t \geq 1$ such that $\liminf_{t\to\infty} \rho_t(2 - \rho_t) > 0$. It is imperative to acknowledge that although their algorithm achieves weak convergence, it is limited to the framework of infinite-dimensional Hilbert spaces. From its inception, equation (1.9) has garnered significant attention owing to its favorable numerical efficacy and uncomplicated structure.

In a recent publication, Yu and Wang [28] introduced a series of novel relaxed CQ algorithms. The fundamental concept underlying these algorithms involves substituting the projections onto the half-spaces C_t and Q_t with the projections onto the intersection of C_t and C_{t-1}, and the intersection of Q_t and Q_{t-1}, respectively. By leveraging the previous half-spaces, the algorithms' convergence rate is enhanced. One of the algorithms proposed by the authors takes the following form:

$$u_{t+1} = P_{C_t^2}\Big(u_t - \tau_t F^*(I - P_{Q_t^2})Fu_t\Big), \tag{1.10}$$

where $C_t^2 = C_t \cap C_{t-1}$, $Q_t^2 = Q_t \cap Q_{t-1}$, and $\tau_t = \frac{\rho_t \|(I-P_{Q_t^2})Fu_t\|^2}{\|F^*(I-P_{Q_t^2})Fu_t\|^2}$ with $\rho_t \subset (0,2)$. They proved that the algorithm (1.10) is a weakly convergent to the solution of the SFP (1.1). In the setting of infinite-dimensional spaces, however, strong convergence is frequently preferable than weak convergence for efficiently solving our problems. This naturally leads to the following question.

Question 1.1. Can we design a strongly convergent iterative scheme for the algorithm (1.10) and extend it for solving the MSSFPMOS (1.2) within the framework of infinite-dimensional real Hilbert spaces?

This paper presents a comprehensive response to Question 1.1, wherein we draw inspiration from the aforementioned works and suggest a strongly convergent relaxed CQ method for effectively solving the MSSFPMOS (1.2) in infinite-dimensional real Hilbert spaces. Our proposed algorithm offers several notable benefits, which are enumerated below.

(1) The algorithm we propose addresses a broader problem, namely the MSSFPMOS (1.2).

(2) The selection of the stepsize is dynamically determined and not contingent upon the operator norm.

(3) We substitute the projection onto the half-space with the projection onto the intersection of two half-spaces. This results in expedited convergence of the algorithm.

(4) The algorithm we propose guarantees a strong convergence to the minimum-norm solution of the MSSFPMOS (1.2).

The subsequent sections of this document are structured as follows. Sect. 2 provides an introduction to fundamental definitions and lemmas that will be utilized throughout the paper. In Sect. 3, a novel iterative method is proposed and its strong convergence is proven. Sect. 4 presents numerical experiments aimed at illustrating the effectiveness of the proposed method.

2. Preliminaries

In this section, we recall some definitions and basic results which are needed in the sequel. Throughout this paper, let

- H, H_1 or H_2 be a real Hilbert space with the inner product $\langle \cdot, \cdot \rangle$, and induced norm $\|\cdot\|$,

- I denote the identity operator on H, H_1 or H_2,
- the symbols " $\rightharpoonup$ " and " $\to$ ", denote the weak and strong convergence, respectively,
- for any sequence $\{u_t\} \subseteq H$, $\omega_w(u_t) = \left\{u \in H : \exists\{u_{t_l}\} \subseteq \{u_t\} \text{ such that } u_{t_l} \rightharpoonup u\right\}$ denotes the weak ω-limit set of $\{u_t\}$.

Definition 2.1. (see [1]) Let $S \subseteq H$ be a non-empty, closed, and convex set. An operator $F : S \to H$ is called

(1) Lipschitz continuous with constant $\theta > 0$ on S if

$$\|Fu - Fv\| \leq \theta\|u - v\|, \ \forall u, v \in S;$$

(2) nonexpansive on S if

$$\|Fu - Fv\| \leq \|u - v\|, \ \forall u, v \in S;$$

(3) firmly nonexpansive on S if

$$\|Fu - Fv\|^2 \leq \|u - v\|^2 - \|(I - F)u - (I - F)v\|^2, \ \forall u, v \in S,$$

which is equivalent to

$$\|Fu - Fv\|^2 \leq \langle Fu - Fv, \ u - v\rangle, \ \forall u, v \in S;$$

(4) θ-inverse strongly monotone ($\theta - ism$) on S if there is $\theta > 0$ such that

$$\langle Fu - Fv, \ u - v\rangle \geq \theta\|Fu - Fv\|^2, \ \forall u, v \in S.$$

Definition 2.2. (see [1]) Let $S \subseteq H$ be a non-empty, closed, and convex set. For each $u \in H$, there is a unique nearest point in S, denoted by $P_S(u)$ such that

$$\|u - P_S(u)\| = \min\{\|u - v\| : v \in S\}.$$

The operator $P_S : H \to S$ is called a metric projection of H onto S.

Lemma 2.3. *(see [1]) Let $S \subseteq H$ be a non-empty, closed, and convex set. The following assertions hold for all $u, v \in H$ and $w \in S$:*

(1) $\langle u - P_S(u), \ w - P_S(u)\rangle \leq 0$;

(2) $\|P_S(u) - P_S(v)\| \leq \|u - v\|$;

(3) $\|P_S(u) - P_S(v)\|^2 \leq \langle P_S(u) - P_S(v), \ u - v\rangle$;

(4) $\|P_S(u) - w\|^2 \leq \|u - w\|^2 - \|u - P_S(u)\|^2$.

From Lemma 2.3, we conclude that the mappings P_S and $I - P_S$ are both $1 - ism$, firmly nonexpansive, and nonexpansive.

Lemma 2.4. *For all $u, v \in H$ and for all $\theta \in \mathbb{R}$, we have*

(1) $\|u \pm v\|^2 \leq \|u\|^2 \pm 2\langle v,\ u+v\rangle$;

(2) $\|u \pm v\|^2 = \|u\|^2 + \|v\|^2 \pm 2\langle u,\ v\rangle$;

(3) $\|\theta u + (1-\theta)v\|^2 = \theta\|u\|^2 + (1-\theta)\|v\|^2 - \theta(1-\theta)\|u-v\|^2$.

Definition 2.5. (see [1]) Let $\phi : H \to (-\infty, +\infty]$ be a given function. Then,

(1) The function ϕ is proper if

$$\{u \in H : \phi(u) < +\infty\} \neq \emptyset.$$

(2) A proper function ϕ is convex if for each $\theta \in (0,1)$,

$$\phi(\theta u + (1-\theta)y) \leq \theta\phi(u) + (1-\theta)\phi(v), \forall u, v \in H.$$

Definition 2.6. Let $\phi : H \to (-\infty, +\infty]$ be a proper function.

(1) A vector $\xi \in H$ is a subgradient of ϕ at a point u if

$$\phi(v) \geq \phi(u) + \langle \xi,\ v-u\rangle,\ \forall v \in H.$$

(2) The set of all subgradients of ϕ at $u \in H$, denoted by $\partial\phi(u)$, is called the subdifferential of ϕ, and

$$\partial\phi(u) = \{\xi \in H : \phi(v) \geq \phi(u) + \langle \xi,\ v-u\rangle,\ \text{for each } v \in H\}. \tag{2.1}$$

(3) If $\partial\phi(u) \neq \emptyset$, ϕ is said to be subdifferentiable at u. If ϕ is continuously differentiable, then

$$\partial\phi(u) = \{\nabla\phi(u)\}.$$

Definition 2.7. Let $\phi : H \to (-\infty, +\infty]$ be a proper function. Then,

(1) ϕ is lower semi-continuous (lsc) at u if $u_t \to u$ implies

$$\phi(u) \leq \liminf_{t\to\infty} \phi(u_t).$$

(2) ϕ is weakly lower semi-continuous (w-lsc) at u if $u_t \rightharpoonup t$ implies

$$\phi(u) \leq \liminf_{t\to\infty} \phi(u_t).$$

(3) ϕ is weakly/lower semi-continuous on H if it is weakly/lower semi-continuous at every point $u \in H$.

Lemma 2.8. *(see [1]) Let $\phi : H \to (-\infty, +\infty]$ be a proper convex function. Then ϕ is lower semi-continuous if and only if it is weakly lower semi-continuous.*

Lemma 2.9. *(see [23]) Let $C \subseteq H_1$ and $Q \subseteq H_2$ be non-empty, closed, and convex sets, and $\phi : H_1 \to (-\infty, +\infty]$ is given by*

$$\phi(u) = \frac{1}{2}\|(I - P_Q)Fu\|^2,$$

where $F : H_1 \to H_2$ is a bounded linear operator. Then, for $\theta > 0$ and $u^* \in H_1$, the following statements are equivalent.

(1) The point u^* solves the SFP (1.1).

(2) $u^* = P_C(u^* - \theta\nabla\phi(u^*))$.

(3) The point u^* solves the variational inequality problem: find a point $w \in C$ such that

$$\langle \nabla\phi(w),\ u - w\rangle \geq 0, \forall u \in C.$$

Lemma 2.10. *(see [3]) Let the function ϕ be given as in Lemma 2.9. Then,*

(1) ϕ is convex and weakly lower semi-continuous on H_1;

(2) $\nabla\phi(u) = F^*(I - P_Q)Fu$, *for* $u \in H_1$;

(3) $\nabla\phi$ is $\|F\|^2$-Lipschitz.

Lemma 2.11. *(see [12]) Let $\{\chi_t\}$ be a non-negative real sequence, such that for all $t \in \mathbb{N}$*

$$\begin{aligned} \chi_{t+1} &\leq (1 - \varrho_t)\chi_t + \varrho_t\mu_t, \\ \chi_{t+1} &\leq \chi_t - \varsigma_t + \varphi_t, \end{aligned} \tag{2.2}$$

where $\{\varrho_t\} \subset (0,1)$, $\{\varsigma_t\}$ is a non-negative, real sequence, and $\{\mu_t\}$ and $\{\varphi_t\}$ are real sequences such that

(1) $\sum_{t=1}^{\infty} \varrho_t = \infty$;

(2) $\lim\limits_{t\to\infty} \varphi_t = 0$;

(3) $\lim\limits_{l\to\infty} \varsigma_{t_l} = 0$ *implies* $\limsup\limits_{l\to\infty} \mu_{t_l} \leq 0$ *for any subsequence $\{t_l\}$ of $\{t\}$.*

Then, $\lim\limits_{t\to\infty} \chi_t = 0$.

3. The Algorithm and its convergence analysis

For simplicity, hereafter, denote $I^* := \{1, 2, \ldots, n\}$ and $J^* := \{1, 2, \ldots, m\}$. We consider the MSSFPMOS (1.2) in which the set C_i $(i \in I^*)$ and the set Q_j $(j \in J^*)$ are defined by

$$C_i = \{u \in H : c_i(u) \leq 0\} \quad \text{and} \quad Q_j = \{v \in H_j : q_j(v) \leq 0\}, \tag{3.1}$$

where $c_i : H \to (-\infty, +\infty]$ for all $i \in I^*$ and $q_j : H_j \to (-\infty, +\infty]$ for all $j \in J^*$ are convex functions. Moreover, we assume (standard assumptions) that

(1) both $c_i (i \in I^*)$ and $q_j (j \in J^*)$ are subdifferentiable on H and H_j, respectively;

(2) for any $u \in H$ and for each $i \in I^*$, a subgradient $\xi_i \in \partial c_i(u)$ can be calculated;

(3) for any $v \in H_j$ and for each $j \in J^*$, a subgradient $\eta_j \in \partial q_j(v)$ can be calculated;

(4) both $\partial c_i (i \in I^*)$ and $\partial q_j (j \in J^*)$ are bounded operators (bounded on bounded sets).

Based on the standard assumptions, the functions $c_i (i \in I^*)$ and $q_j (j \in J^*)$ are clearly lower semi-continuous. Moreover, since $c_i (i \in I^*)$ and $q_j (j \in J^*)$ are also convex, it then follows from Lemma 2.8 that $c_i (i \in I^*)$ and $q_j (j \in J^*)$ are weakly lower semi-continuous. In our algorithm, given the t^{th} iterative point u_t, we construct "n" sets C_i^t $(i \in I^*)$ which contains the original sets C_i $(i \in I^*)$ and "m" sets Q_j^t $(j \in J^*)$ which contains the original sets Q_j $(j \in J^*)$, as follows. The set C_i^t $(i \in I^*)$ is constructed as

$$C_i^t = \Big\{ u \in H : c_i(u_t) + \langle \xi_i^t,\ u - u_t \rangle \leq 0 \}, \tag{3.2}$$

where $\xi_i^t \in \partial c_i(u_t)$ and it follows from the fact that $C_i^t \supseteq C_i \neq \emptyset$ $(i \in I^*)$ the set C_i^t is non-empty (see in [29]). The set Q_j^t $(j \in J^*)$ is defined as

$$Q_j^t = \Big\{ v \in H_j : q_j(F_j u_t) + \langle \eta_j^t,\ v - F_j u_t \rangle \leq 0 \Big\}, \tag{3.3}$$

where $\eta_j^t \in \partial q_j(F_j u_t)$. Indeed, Q_j^t is non-empty because $Q_j^t \supseteq Q_j \neq \emptyset$ $(j \in J^*)$. Therefore, both C_i^t and Q_j^t are nothing but non-empty half-spaces and it is easy to verify that (see [29]) $C_i^t \supseteq C_i$ $(i \in I^*)$ and $Q_j^t \supseteq Q_j$ $(j \in J^*)$ hold for every $t \geq 0$.

Note that in contrast to an algorithm that involves metric projections onto the given sets C_i and Q_j, which is more complex, an algorithm that utilizes metric projections onto the half-spaces C_i^t and Q_j^t defined in (3.2) and (3.3) is easier to implement due to the explicit formula for projecting onto a half-space. In this case, at each step t, the algorithm only needs to compute a projection onto the current sets C_i^t and Q_j^t, rather than utilizing the previous half-spaces in their entirety. This article draws inspiration from the works of Yu and Wang [28]. Our proposed algorithm replaces the projections to the half-spaces C_i^t and Q_j^t with the projections to the intersection of C_i^t and C_i^{t-1}, and the intersection of Q_j^t and Q_j^{t-1}, respectively. This modification enables us to make full use of the previous half-spaces, resulting in a faster convergence rate of our algorithm. Furthermore, we introduce a dynamically chosen stepsize that is not reliant on the operator norm.

We hereby introduce a highly effective self-adaptive relaxed CQ method that exhibits strong convergence properties for solving the MSSFPMOS (1.2) within the context of infinite-

dimensional real Hilbert spaces.

Algorithm 1: A self-adaptive approximation technique for MSSFPMOS (1.2)

Step 0. Choose two sequences $\{\sigma_t\} \subset (0,1)$ and $\{\rho_t\} \subset (0,2)$ and select $\beta > 0$. Let $u_0 \in H$ be arbitrary initial guess and set $t := 0$. Take the weights α_i^t $(i \in I^*) > 0$ and the constant parameters β_j $(j \in J^*) > 0$ such that

$$\sum_{i=1}^{n} \alpha_i^t = 1 \quad \text{and} \quad \inf_{i \in I_t} \alpha_i^t > \alpha > 0, \text{ where } I_t = \{i \in I^* : \alpha_i^t > 0\}, \quad \text{and} \quad \sum_{j=1}^{m} \beta_j = 1.$$

Step 1. Given the current iterate u_t, compute the next iterate u_{t+1} via the formula

$$u_{t+1} = \sum_{i=1}^{n} \alpha_i^t P_{C_{i,t}^{int}} \left((1-\sigma_t)\Big(u_t - \tau_t \sum_{j=1}^{m} \beta_j F_j^* \Big(I - P_{Q_{j,t}^{int}} \Big) F_j u_t \Big) \right)$$

where $C_{i,t}^{int}$, $Q_{j,t}^{int}$, and τ_t are respectively defined as follows:

$$C_{i,t}^{int} = C_i^t \cap C_i^{t-1}, \text{ for each } i = 1, 2, \dots, n,$$
$$Q_{j,t}^{int} = Q_j^t \cap Q_j^{t-1}, \text{ for each } j = 1, 2, \dots, m,$$

and

$$\tau_t := \frac{\rho_t \sum_{j=1}^{m} \beta_j \left\| \Big(I - P_{Q_{j,t}^{int}} \Big) F_j u_t \right\|^2}{\left(\max\left\{ \beta, \ \left\| \sum_{j=1}^{m} \beta_j F_j^* \Big(I - P_{Q_{j,t}^{int}} \Big) F_j u_t \right\| \right\} \right)^2}. \tag{3.4}$$

Step 2. If $u_{t+1} = u_t$, then stop; otherwise, set $t := t + 1$ and return to **Step 1.**

Remark 3.1. Since C_i^t, C_i^{t-1} for each $i \in I^*$ and Q_j^t, Q_j^{t-1} for each $j \in J^*$ are both half-spaces, $C_{i,t}^{int}$ and $Q_{j,t}^{int}$ are both intersection of two half-spaces. From the subdifferentiable inequality (2.1), it is clear that $C_i \subseteq C_i^{t-1}$, $C_i \subseteq C_i^t$ for each $i \in I^*$ and $Q_j \subseteq Q_j^{t-1}$, $Q_j \subseteq Q_j^t$ for each $j \in J^*$. Hence, we have $C_i \subseteq C_{i,t}^{int}$ for each $i \in I^*$ and $Q_j \subseteq Q_{j,t}^{int}$ for each $j \in J^*$. Moreover, the explicit formula for projecting onto the intersection of two half-spaces can be found in [1], making the implementation of Algorithm 1 a straightforward task.

Theorem 3.2. *Assume that the set of solutions Ω of the MSSFPMOS (1.2) is non-empty and suppose that the sequences $\{\sigma_t\}$ and $\{\rho_t\}$ in Algorithm 1 satisfy the conditions:*

(a1) $\{\sigma_t\} \subset (0,1)$ *such that* $\lim_{t\to\infty} \sigma_t = 0$ *and* $\sum_{t=0}^{\infty} \sigma_t = \infty$,

(a2) $\{\rho_t\} \subset (0,2)$ *such that* $\liminf_{t\to\infty} \rho_t(2-\rho_t) > 0$.

Then, the sequence $\{u_t\}$ generated by Algorithm 1 converges strongly to an element $u^* \in \Omega$, where $u^* = P_\Omega 0$.

Proof. Let $u^* \in \Omega$. Since $C_i \subseteq C_{i,t}^{int}$ for each $i \in I^*$, then $u^* = P_{C_i}u^* = P_{C_{i,t}^{int}}u^*$. Let

$$v_t = (1-\sigma_t)\Big(u_t - \tau_t \sum_{j=1}^{m} \beta_j F_j^* \Big(I - P_{Q_{j,t}^{int}}\Big) F_j u_t\Big)$$

for all $i \in I^*$. Since $P_{C_{i,t}^{int}}$ for each $i \in I^*$ is firmly nonexpansive, we get

$$\begin{aligned}
\|u_{t+1} - u^*\|^2 &= \Big\| \sum_{i=1}^{n} \alpha_i^t \Big(P_{C_{i,t}^{int}} v_t - u^* \Big) \Big\|^2 \\
&\leq \sum_{i=1}^{n} \alpha_i^t \Big\| P_{C_{i,t}^{int}} v_t - u^* \Big\|^2 \\
&\leq \sum_{i=1}^{n} \alpha_i^t \Big(\|v_t - u^*\|^2 - \Big\| (I - P_{C_{i,t}^{int}}) v_t \Big\|^2 \Big) \\
&= \|v_t - u^*\|^2 - \sum_{i=1}^{n} \alpha_i^t \Big\| (I - P_{C_{i,t}^{int}}) v_t \Big\|^2 \\
&= \Big\| (1-\sigma_t)\Big(u_t - \tau_t \sum_{j=1}^{m} \beta_j F_j^* \Big(I - P_{Q_{j,t}^{int}}\Big) F_j u_t\Big) - u^* \Big\|^2 \\
&\quad - \sum_{i=1}^{n} \alpha_i^t \Big\| (I - P_{C_{i,t}^{int}}) v_t \Big\|^2 \\
&= \Big\| \sigma_t(-u^*) + (1-\sigma_t)\Big(u_t - \tau_t \sum_{j=1}^{m} \beta_j F_j^* \Big(I - P_{Q_{j,t}^{int}}\Big) F_j u_t - u^*\Big) \Big\|^2 \\
&\quad - \sum_{i=1}^{n} \alpha_i^t \Big\| (I - P_{C_{i,t}^{int}}) v_t \Big\|^2 \\
&\leq \sigma_t \|u^*\|^2 + (1-\sigma_t) \Big\| u_t - \tau_t \sum_{j=1}^{m} \beta_j F_j^* \Big(I - P_{Q_{j,t}^{int}}\Big) F_j u_t - u^* \Big\|^2 \\
&\quad - \sum_{i=1}^{n} \alpha_i^t \Big\| (I - P_{C_{i,t}^{int}}) v_t \Big\|^2. \qquad (3.5)
\end{aligned}$$

Since $Q_j \subseteq Q_{j,t}^{int}$ for each $j \in J^*$, then $F_j u^* = P_{Q_j} F_j u^* = P_{Q_{j,t}^{int}} F_j u^*$. Note that for each $j \in J^*$, $I - P_{Q_{j,t}^{int}}$ is $1-ism$ and $\sum_{j=1}^{m} \beta_j F_j^* \Big(I - P_{Q_{j,t}^{int}}\Big) F_j u^* = 0$, it means for each $j \in J^*$ that

$$\begin{aligned}
&\Big\langle \sum_{j=1}^{m} \beta_j F_j^* \Big(I - P_{Q_{j,t}^{int}}\Big) F_j u_t,\ u_t - u^* \Big\rangle \\
&= \sum_{j=1}^{m} \beta_j \Big\langle F_j^* \Big(I - P_{Q_{j,t}^{int}}\Big) F_j u_t,\ u_t - u^* \Big\rangle \\
&= \sum_{j=1}^{m} \beta_j \Big\langle \Big(I - P_{Q_{j,t}^{int}}\Big) F_j u_t - \Big(I - P_{Q_{j,t}^{int}}\Big) F_j u^*,\ F_j u_t - F_j u^* \Big\rangle
\end{aligned}$$

$$\geq \sum_{j=1}^{m} \beta_j \left\| \left(I - P_{Q_{j,t}^{int}}\right) F_j u_t \right\|^2. \tag{3.6}$$

Set $\Xi_t := \max\left\{\beta, \left\|\sum_{j=1}^{m} \beta_j F_j^* \left(I - P_{Q_{j,t}^{int}}\right) F_j u_t\right\|\right\}$. This implies $\left\|\sum_{j=1}^{m} \beta_j F_j^* \left(I - P_{Q_{j,t}^{int}}\right) F_j u_t\right\| \leq \Xi_t$. This together with (3.6) gives that

$$\begin{aligned}
&\left\| u_t - \tau_t \sum_{j=1}^{m} \beta_j F_j^* \left(I - P_{Q_{j,t}^{int}}\right) F_j u_t - u^* \right\|^2 \\
= &\left\| (u_t - u^*) - \tau_t \sum_{j=1}^{m} \beta_j F_j^* \left(I - P_{Q_{j,t}^{int}}\right) F_j u_t \right\|^2 \\
\leq &\|u_t - u^*\|^2 + \tau_t^2 \left\| \sum_{j=1}^{m} \beta_j F_j^* \left(I - P_{Q_{j,t}^{int}}\right) F_j u_t \right\|^2 \\
&-2\tau_t \left\langle \sum_{j=1}^{m} \beta_j F_j^* \left(I - P_{Q_{j,t}^{int}}\right) F_j u_t,\ u_t - u^* \right\rangle \\
\leq &\|u_t - u^*\|^2 + \tau_t^2 \Xi_t^2 - 2\tau_t \sum_{j=1}^{m} \beta_j \left\| \left(I - P_{Q_{j,t}^{int}}\right) F_j u_t \right\|^2 \\
= &\|u_t - u^*\|^2 - \rho_t(2-\rho_t) \frac{\left(\sum_{j=1}^{m} \beta_j \left\| \left(I - P_{Q_{j,t}^{int}}\right) F_j u_t \right\|^2 \right)^2}{\Xi_t^2}.
\end{aligned} \tag{3.7}$$

Substituting, (3.7) into (3.5), we get

$$\begin{aligned}
\|u_{t+1} - u^*\|^2 \leq\ & \sigma_t \|u^*\|^2 + (1-\sigma_t)\|u_t - u^*\|^2 \\
&-\rho_t(2-\rho_t)(1-\sigma_t) \frac{\left(\sum_{j=1}^{m} \beta_j \left\| \left(I - P_{Q_{j,t}^{int}}\right) F_j u_t \right\|^2 \right)^2}{\Xi_t^2} \\
&-\sum_{i=1}^{n} \alpha_i^t \left\| (I - P_{C_{i,t}^{int}}) v_t \right\|^2.
\end{aligned} \tag{3.8}$$

By (a1) and (a2), we obtain from (3.8) that

$$\begin{aligned}
\|u_{t+1} - u^*\|^2 &\leq \sigma_t \|u^*\|^2 + (1-\sigma_t)\|u_t - u^*\|^2 \\
&\leq \max\left\{\|u^*\|^2,\ \|u_t - u^*\|^2\right\} \\
&\ \ \vdots \\
&\leq \max\left\{\|u^*\|^2,\ \|u_0 - u^*\|^2\right\}.
\end{aligned} \tag{3.9}$$

For that reason, the sequence $\{\|u_t - u^*\|\}_{t=0}^{t=\infty}$ is bounded. As a consequence, $\{u_t\}_{t=0}^{t=\infty}$ and $\{F_j u_t\}_{t=0}^{t=\infty}$ for each $j \in J^*$ are bounded.

By (a2), we obtain from (3.7) that

$$\left\| u_t - \tau_t \sum_{j=1}^{m} \beta_j F_j^* \left(I - P_{Q_{j,t}^{int}} \right) F_j u_t - u^* \right\|^2 \leq \|u_t - u^*\|^2. \tag{3.10}$$

By Lemma 2.3, we also obtain the following estimation.

$$\begin{aligned}
& \|u_{t+1} - u^*\|^2 \\
= & \left\| \sum_{i=1}^{n} \alpha_i^t P_{C_{i,t}^{int}}(v_t) - u^* \right\|^2 \\
= & \left\| \sum_{i=1}^{n} \alpha_i^t P_{C_{i,t}^{int}}(v_t) - \sum_{i=1}^{n} \alpha_i^t P_{C_{i,t}^{int}}(u^*) \right\|^2 \\
\leq & \left\| v_t - u^* \right\|^2 \\
= & \left\| (1-\sigma_t)\left(u_t - \tau_t \sum_{j=1}^{m} \beta_j F_j^* \left(I - P_{Q_{j,t}^{int}} \right) F_j u_t \right) - u^* \right\|^2 \\
= & \left\| (1-\sigma_t)\left(u_t - \tau_t \sum_{j=1}^{m} \beta_j F_j^* \left(I - P_{Q_{j,t}^{int}} \right) F_j u_t - u^* \right) - \sigma_t u^* \right\|^2 \\
\leq & (1-\sigma_t) \left\| u_t - \tau_t \sum_{j=1}^{m} \beta_j F_j^* \left(I - P_{Q_{j,t}^{int}} \right) F_j u_t - u^* \right\|^2 + \sigma_t \|u^*\|^2.
\end{aligned} \tag{3.11}$$

From (3.11), we also get

$$\begin{aligned}
\|u_{t+1} - u^*\|^2 \leq & \left\| (1-\sigma_t)\left(u_t - \tau_t \sum_{j=1}^{m} \beta_j F_j^* \left(I - P_{Q_{j,t}^{int}} \right) F_j u_t \right) - u^* \right\|^2 \\
= & \left\| \sigma_t(-u^*) + (1-\sigma_t)\left(u_t - \tau_t \sum_{j=1}^{m} \beta_j F_j^* \left(I - P_{Q_{j,t}^{int}} \right) F_j u_t - u^* \right) \right\|^2 \\
= & \sigma_t^2 \|u^*\|^2 + (1-\sigma_t)^2 \left\| u_t - \tau_t \sum_{j=1}^{m} \beta_j F_j^* \left(I - P_{Q_{j,t}^{int}} \right) F_j u_t - u^* \right\|^2 \\
+ & 2\sigma_t(1-\sigma_t) \left\langle u_t - \tau_t \sum_{j=1}^{m} \beta_j F_j^* \left(I - P_{Q_{j,t}^{int}} \right) F_j u_t - u^*, \ -u^* \right\rangle.
\end{aligned} \tag{3.12}$$

By combining (3.10) and (3.12), we obtain that

$$\begin{aligned}
\|u_{t+1} - u^*\|^2 \leq & \sigma_t^2 \|u^*\|^2 + (1-\sigma_t)^2 \|u_t - u^*\|^2 + 2\sigma_t(1-\sigma_t)\langle u_t - u^*, \ -u^* \rangle \\
+ & 2\sigma_t\tau_t(1-\sigma_t) \left\langle \sum_{j=1}^{m} \beta_j F_j^* \left(I - P_{Q_{j,t}^{int}} \right) F_j u_t, \ u^* \right\rangle \\
\leq & (1-\sigma_t)\|u_t - u^*\|^2 + \sigma_t \Big[\sigma_t \|u^*\|^2 + 2(1-\sigma_t)\langle u_t - u^*, \ -u^* \rangle \\
+ & 2\tau_t(1-\sigma_t) \left\langle \sum_{j=1}^{m} \beta_j F_j^* \left(I - P_{Q_{j,t}^{int}} \right) F_j u_t, \ u^* \right\rangle \Big]
\end{aligned}$$

$$\begin{aligned} &\leq (1-\sigma_t)\|u_t-u^*\|^2+\sigma_t\Big[\sigma_t\|u^*\|^2+2(1-\sigma_t)\langle u_t-u^*,\ -u^*\rangle \\ &+ 2\tau_t(1-\sigma_t)\Big\|\sum_{j=1}^{m}\beta_j F_j^*\Big(I-P_{Q_{j,t}^{int}}\Big)F_j u_t\Big\|\|u^*\|\Big]. \end{aligned} \tag{3.13}$$

Subsequently, we demonstrate that the sequence $\{u_t\}$ produced by Algorithm 1 converges strongly to the minimum norm element $u^*=P_\Omega 0$.

Let $u^*=P_\Omega 0$. Based on (a1) and (a2), without loss of generality, we can assume that $\exists\kappa>0$ such that $\rho_t(2-\rho_t)(1-\sigma_t)\geq\kappa$ for all $t\in\mathbb{N}$. Hence, we obtain from (3.8) that

$$\begin{aligned} \|u_{t+1}-u^*\|^2 \quad &\leq \quad \sigma_t\|u^*\|^2+\|u_t-u^*\|^2-\kappa\frac{\Big(\sum_{j=1}^{m}\beta_j\Big\|\Big(I-P_{Q_{j,t}^{int}}\Big)F_j u_t\Big\|^2\Big)^2}{\Xi_t^2} \\ &\quad -\sum_{i=1}^{n}\alpha_i^t\Big\|(I-P_{C_{i,t}^{int}})v_t\Big\|^2. \end{aligned} \tag{3.14}$$

Using (3.13) and (3.14), for all $t\in\mathbb{N}$, we derive the two inequalities in (3.15):

$$\begin{aligned} &\|u_{t+1}-u^*\|^2\leq(1-\sigma_t)\|u_t-u^*\|^2+\sigma_t\mu_t, \\ &\|u_{t+1}-u^*\|^2\leq\|u_t-u^*\|^2-\varsigma_t+\sigma_t\|u^*\|^2. \end{aligned} \tag{3.15}$$

Now, relating (3.15) to (2.2), we obtain the following settings for all positive integer t:

$$\begin{aligned} &\chi_t=\|u_t-u^*\|^2; \\ &\mu_t=\sigma_t\|u^*\|^2+2(1-\sigma_t)\langle u_t-u^*,\ -u^*\rangle+2\tau_t(1-\sigma_t)\Big\|\textstyle\sum_{j=1}^{m}\beta_j F_j^*\Big(I-P_{Q_{j,t}^{int}}\Big)F_j u_t\Big\|\|u^*\|; \\ &\varsigma_t:=\kappa\frac{\Big(\sum_{j=1}^{m}\beta_j\Big\|\Big(I-P_{Q_{j,t}^{int}}\Big)F_j u_t\Big\|^2\Big)^2}{\Xi_t^2}+\textstyle\sum_{i=1}^{n}\alpha_i^t\Big\|(I-P_{C_{i,t}^{int}})v_t\Big\|^2 \end{aligned} \tag{3.16}$$

Furthermore, set $\varrho_t:=\sigma_t$, $\varphi_t:=\sigma_t\|u^*\|^2$ and thus $\{\varrho_t\}\subset(0,1)$, $\lim\limits_{t\to\infty}\varrho_t=0$, $\sum\limits_{t=0}^{\infty}\varrho_t=\infty$, $\lim\limits_{t\to\infty}\varphi_t=0$.

To utilize Lemma 2.11 for the convergence analysis of the sequence $\{\chi_t\}$, it suffices to illustrate that for any subsequence $\{t_l\}$ of $\{t\}$

$$\lim_{l\to\infty}\varsigma_{t_l}=0 \text{ implies } \limsup_{l\to\infty}\mu_{t_l}\leq 0.$$

Let $\{t_l\}$ be a subsequence of $\{t\}$ and suppose $\lim\limits_{l\to\infty}\varsigma_{t_l}=0$. Then, we have

$$\lim_{l\to\infty}\left[\kappa\frac{\Big(\sum_{j=1}^{m}\beta_j\Big\|\Big(I-P_{Q_{j,t_l}^{int}}\Big)F_j u_{t_l}\Big\|^2\Big)^2}{\Xi_{t_l}^2}+\sum_{i=1}^{n}\alpha_i^t\Big\|(I-P_{C_{i,t_t}^{int}})v_{t_l}\Big\|^2\right]=0. \tag{3.17}$$

Since $\kappa > 0$, (3.17) implies that

$$\lim_{l\to\infty} \frac{\left(\sum_{j=1}^{m} \beta_j \left\| \left(I - P_{Q_{j,t_l}^{int}}\right) F_j u_{t_l} \right\|^2\right)^2}{\Xi_{t_l}^2} = 0, \tag{3.18}$$

and

$$\lim_{l\to\infty} \left\| (I - P_{C_{i,t_l}^{int}}) v_{t_l} \right\|^2 = 0. \tag{3.19}$$

Since $I - P_{Q_{j,t_l}^{int}}$ for each $j \in J^*$ is nonexpansive, $\{u_{t_l}\}$ is bounded, and F_j for each $j \in J^*$ is a bounded linear operator, the sequence $\{\left\| \left(I - P_{Q_{j,t_l}^{int}}\right) F_j u_{t_l} \right\|\}$ for each $j \in J^*$ is bounded, and thus the sequence $\{\Xi_{t_l}\}$ is bounded. Hence, we obtain from (3.18) that

$$\lim_{l\to\infty} \sum_{j=1}^{m} \beta_j \left\| \left(I - P_{Q_{j,t_l}^{int}}\right) F_j u_{t_l} \right\| = 0. \tag{3.20}$$

Next, we prove that each weak cluster point of $\{u_{t_l}\}$ belongs to Ω, that is $\omega_w(u_{t_l}) \subseteq \Omega$. Let $\bar{u} \in H$ be a weak cluster point of $\{u_{t_l}\}$. Since $\{u_{t_l}\}$ is bounded, we may assume that there exists a subsequence $\{u_{t_{l_r}}\}$ of $\{u_{t_l}\}$ that weakly convergent to $\bar{u}$. Furthermore, since each F_j for each $j \in J^*$ is linear and bounded, this yields that $\{F_j u_{t_{l_r}}\}$ weakly converges to $F_j\bar{u}$. We claim here that $\bar{u} \in \Omega$. To show this, it suffices to show that $\bar{u} \in C_i$ for all $i \in I^*$ and $F_j\bar{u} \in Q_j$ for all $j \in J^*$.

Firstly, we show that $F_j\bar{u} \in Q_j$ for all $j \in J^*$. Since ∂q_j for each $j \in J^*$ is bounded on bounded set, we may assume that there is a constant $\mathring{\eta} > 0$ such that $\|\eta_j^{t_{l_r}}\| \leq \mathring{\eta}$, where $\eta_j^{t_{l_r}} \in \partial q_j(F_j u_{t_{l_r}})$ for each $j \in J^*$. That is the sequence $\{\eta_j^{t_{l_r}}\}$ is bounded. Since $P_{Q_{j,t_{l_r}}^{int}}(F_j u_{t_{l_r}}) \in Q_{j,t_{l_r}}^{int} \subseteq Q_j^{t_{l_r}}$ for each $j \in J^*$, it follows from (3.3) and (3.20) for all $j \in J^*$ and as $r \to \infty$ that

$$\begin{aligned} q_j\left(F_j u_{t_{l_r}}\right) \leq \left\langle \eta_j^{t_{l_r}},\ F_j u_{t_{l_r}} - P_{Q_{j,t_{l_r}}^{int}}(F_j u_{t_{l_r}}) \right\rangle &\leq \left\|\eta_j^{t_{l_r}}\right\| \left\| \left(I - P_{Q_{j,t_{l_r}}^{int}}\right) F_j u_{t_{l_r}} \right\| \\ &\leq \mathring{\eta} \left\| \left(I - P_{Q_{j,t_{l_r}}^{int}}\right) F_j u_{t_{l_r}} \right\| \to 0. \end{aligned} \tag{3.21}$$

The weakly lower semi-continuity of q_j together with (3.21) implies for all $j \in J^*$ that

$$q_j(F_j\bar{u}) \leq \liminf_{r\to\infty} q_j\left(F_j u_{t_{l_r}}\right) \leq \lim_{r\to\infty} \mathring{\eta} \left\| \left(I - P_{Q_{j,t_{l_r}}^{int}}\right) F_j u_{t_{l_r}} \right\| = 0. \tag{3.22}$$

It turns out that, $F_j\bar{u} \in Q_j$, for all $j \in J^*$.

Next, we prove that $\bar{u} \in C_i$ for all $i \in I^*$. By (a1) and (3.18), we obtain that

$$\begin{aligned} \|v_{t_{l_r}} - u_{t_{l_r}}\|^2 &\leq \left\| (1 - \sigma_{t_{l_r}}) \left(u_{t_{l_r}} - \tau_{t_{l_r}} \sum_{j=1}^{m} \beta_j F_j^* \left(I - P_{Q_{j,t_{l_r}}^{int}}\right) F_j u_{t_{l_r}} \right) - u_{t_{l_r}} \right\|^2 \\ &= \left\| \sigma_{t_{l_r}}(-u_{t_{l_r}}) + (1 - \sigma_t) \left(u_{t_{l_r}} - \tau_{t_{l_r}} \sum_{j=1}^{m} \beta_j F_j^* \left(I - P_{Q_{j,t}^{int}}\right) F_j u_{t_{l_r}} - u_{t_{l_r}} \right) \right\|^2 \end{aligned}$$

$$\begin{aligned} &\leq \sigma_{t_{l_r}}\left\|u_{t_{l_r}}\right\|^2+(1-\sigma_{t_{l_r}})\tau_{t_{l_r}}^2\left\|\sum_{j=1}^{m}\beta_j F_j^*\left(I-P_{Q_{j,t}^{int}}\right)F_j u_{t_{l_r}}\right\|^2 \\ &\leq \sigma_{t_{l_r}}\left\|u_{t_{l_r}}\right\|^2+(1-\sigma_{t_{l_r}})\rho_{t_{l_r}}^2\frac{\left(\sum_{j=1}^{m}\beta_j\left\|\left(I-P_{Q_{j,t_{l_r}}^{int}}\right)F_j u_{t_{l_r}}\right\|^2\right)^2}{\Xi_{t_{l_r}}^2}\to 0 \end{aligned} \tag{3.23}$$

as $r\to\infty$, that is

$$\lim_{r\to\infty}\left\|v_{t_{l_r}}-u_{t_{l_r}}\right\|=0. \tag{3.24}$$

In fact, since $P_{C_{i,t_{l_r}}^{int}}(u_{t_{l_r}})\in C_{i,t_{l_r}}^{int}\subseteq C_i^{t_{l_r}}$ for each $i\in I^*$, it follows from (3.3) for all $i\in I^*$ that

$$\begin{aligned} c_i(u_{t_{l_r}}) &\leq \left\langle \xi_i^{t_{l_r}},\ u_{t_{l_r}}-P_{C_{i,t_{l_r}}^{int}}(v_{t_{l_r}})\right\rangle \\ &= \left\langle \xi_i^{t_{l_r}},\ (u_{t_{l_r}}-v_{t_{l_r}})+\left(I-P_{C_{i,t_{l_r}}^{int}}\right)v_{t_{l_r}}\right\rangle \\ &= \left\langle \xi_i^{t_{l_r}},\ (u_{t_{l_r}}-v_{t_{l_r}})\right\rangle+\left\langle \xi_i^{t_{l_r}},\ \left(I-P_{C_{i,t_{l_r}}^{int}}\right)v_{t_{l_r}}\right\rangle \\ &\leq \left\|\xi_i^{t_{l_r}}\right\|\left[\left\|u_{t_{l_r}}-v_{t_{l_r}}\right\|+\left\|\left(I-P_{C_{i,t_{l_r}}^{int}}\right)v_{t_{l_r}}\right\|\right]. \end{aligned} \tag{3.25}$$

Since ∂c_i for each $i\in I^*$ is bounded on bounded set, we may again assume that for all $t_{l_r}\geq 0$, there is a constant $\mathring{\xi}>0$ such that $\|\xi_i^{t_{l_r}}\|\leq\mathring{\xi}$, where $\xi_i^{t_{l_r}}\in\partial c_i(u_{t_{l_r}})$ for each $i\in I^*$. Hence, it follows from (3.19), (3.24), and (3.25) for all $i\in I^*$ as $r\to\infty$ that

$$\begin{aligned} c_i(u_{t_{l_r}}) &\leq \left\|\xi_i^{t_{l_r}}\right\|\left[\left\|u_{t_{l_r}}-v_{t_{l_r}}\right\|+\left\|\left(I-P_{C_{i,t_{l_r}}^{int}}\right)v_{t_{l_r}}\right\|\right] \\ &\leq \mathring{\xi}\left[\left\|u_{t_{l_r}}-v_{t_{l_r}}\right\|+\left\|\left(I-P_{C_{i,t_{l_r}}^{int}}\right)v_{t_{l_r}}\right\|\right]\to 0. \end{aligned} \tag{3.26}$$

The weakly lower semi-continuity of c_i together with (3.26) implies for all $i\in I^*$ that

$$c_i(\bar{u})\leq\liminf_{r\to\infty}c_i(u_{t_{l_r}})\leq 0, \tag{3.27}$$

consequently, $\bar{u}\in C_i$, $\forall i\in I^*$. Altogether, we conclude that $\bar{u}\in\Omega$. Since $\bar{u}$ is arbitrary, we conclude that each weak cluster point of $\{u_{t_l}\}$ belongs to Ω. That is $w_\omega(u_{t_l})\subseteq\Omega$. This implies there exists a subsequence $\{u_{t_{l_r}}\}$ of $\{u_{t_l}\}$ such that $u_{t_{l_r}}\rightharpoonup\bar{u}$.

In addition, from Lemma 2.3 (1) and (a1), we obtain that

$$\begin{aligned} \limsup_{r\to\infty}\mu_{t_{l_r}} &= \limsup_{r\to\infty}\left[\sigma_{t_{l_r}}\|u^*\|^2+2(1-\sigma_{t_{l_r}})\langle u_{t_{l_r}}-u^*,\ -u^*\rangle\right. \\ &+ \left.2\tau_{t_{l_r}}(1-\sigma_{t_{l_r}})\left\|\sum_{j=1}^{m}\beta_j F_j^*\left(I-P_{Q_{j,t_{l_r}}^{int}}\right)F_j u_{t_{l_r}}\right\|\|u^*\|\right] \\ &= 2\limsup_{r\to\infty}\langle u_{t_{l_r}}-u^*,\ -u^*\rangle \end{aligned}$$

$$\begin{aligned} &= 2 \max_{\bar{u}\in\omega_w(u_{t_{l_r}})} \langle \bar{u} - u^*, \ -u^* \rangle \\ &\leq 0. \end{aligned} \tag{3.28}$$

Therefore, from Lemma 2.11, we conclude that any sequence $\{u_t\}$ generated by Algorithm 1 converges strongly to the minimum-norm element $u^* = P_\Omega 0$. The proof is complete. ∎

3.1. Corollaries

It is readily seen that, for the case where $n = 1$, the MSSFPMOS (1.2) reduced to the following problem: introduced and studied by Reich et al. [17] in infinite-dimensional Hilbert spaces.

Let H, H_j, $j = 1, 2, \dots, m$, be real Hilbert spaces and let $F_j : H \to H_j$, $j = 1, 2, \dots, m$, be bounded linear operators. The split feasibility problem with multiple output sets (SFPMOS, for short) is to find a point u^* such that

$$u^* \in \Gamma := C \cap \Big(\cap_{j=1}^{m} F_j^{-1}(Q_j) \Big) \neq \emptyset, \tag{3.29}$$

where C and Q_j, $j = 1, 2, \dots, m$, are non-empty, closed and convex subsets of H and H_j, $j = 1, 2, \dots, m$, respectively.

Reich et al. [17] introduced the following two approximation iterative methods for solving the SFPMOS (3.29). For any given point $u_0 \in H$, $\{u_t\}$ is a sequence generated by

$$u_{t+1} := P_C\Big(u_t - \tau_t \sum_{j=1}^{m} F_j^*(I - P_{Q_j})F_j u_t\Big) \tag{3.30}$$

and for any initial point $v_0 \in H$, $\{v_t\}$ is a sequence generated by

$$v_{t+1} := \sigma_t f(v_t) + (1 - \sigma_t)P_C\Big(v_t - \tau_t \sum_{j=1}^{m} F_j^*(I - P_{Q_j})F_j v_t\Big), \tag{3.31}$$

where $f : C \to C$ is a $\theta \in [0, 1)$-strict contraction mapping of H into itself, $\tau_t \in (0, \infty)$ and $\{\sigma_t\} \subset (0, 1)$. It was proved that, if the sequence $\{\tau_t\}$ satisfies the condition:

$$0 < a \leq \tau_t \leq b < \frac{2}{m \max_{j=1,2,\dots,m}\{\|F_j\|^2\}}$$

for all $t \geq 1$, then the sequence $\{u_t\}$ generated by (3.30) converges weakly to a solution point $u^* \in \Gamma$ of the SFPMOS (3.29). Furthermore, if the sequence $\{\sigma_t\}$ satisfies the conditions:

$$\lim_{t\to\infty} \sigma_t = 0 \quad \text{and} \quad \sum_{t=1}^{\infty} \sigma_t = \infty,$$

then the sequence $\{v_t\}$ generated by (3.31) converges strongly to a solution point $u^* \in \Gamma$ of the SFPMOS (3.29), which is a unique solution of the variational inequality

$$\langle (I - f)u^*, u - u^* \rangle \geq 0 \ \forall u \in \Gamma.$$

Note that the iterative methods given by (3.30) and (3.31) require to compute the metric projections on to the sets C and Q_j and need to compute the operator norm, in which is difficult to do so.

If $n = 1$ in the MSSFPMOS (1.2), accordingly in Algorithm 1, as an immediate consequence of Theorem 3.2, we obtain the following result which solves the SFPMOS (3.29).

Corollary 3.3. *Assume that the set of solutions Γ of the SFPMOS (3.29) is non-empty and suppose that the sequences $\{\sigma_t\}$ and $\{\rho_t\}$ in Algorithm 2 satisfy the assumptions (a1) and (a2) in Theorem 3.2. Then, the sequence $\{u_t\}$ generated by Algorithm 2 converges strongly to an element $u^* \in \Gamma$, where $u^* = P_\Gamma 0$.*

Algorithm 2: A self-adaptive approximation technique for SFPMOS (3.29)

Step 0. *Choose two sequences $\{\sigma_t\} \subset (0,1)$ and $\{\rho_t\} \subset (0,2)$ and select $\beta > 0$. Let $u_0 \in H$ be arbitrary initial guess and set $t := 0$. Take the constant parameters β_j $(j = 1, 2, \dots, m) > 0$ such that $\sum_{j=1}^{m} \beta_j = 1$.*

Step 1. *Given the current iterate u_t, compute the next iterate u_{t+1} via the formula*

$$u_{t+1} = P_{C_t^2}\Big((1-\sigma_t)\big(u_t - \tau_t \sum_{j=1}^{m} \beta_j F_j^*\big(I - P_{Q_{j,t}^{int}}\big)F_j u_t\big)\Big),$$

where $C_t^2 = C_t \cap C_{t-1}$, $Q_{j,t}^{int} = Q_j^t \cap Q_j^{t-1}$ for each $j = 1, 2, \dots, m$, and

$$\tau_t := \frac{\rho_t \sum_{j=1}^{m} \beta_j \big\|\big(I - P_{Q_{j,t}^{int}}\big)F_j u_t\big\|^2}{\left(max\Big\{\beta,\ \big\|\sum_{j=1}^{m} \beta_j F_j^*\big(I - P_{Q_{j,t}^{int}}\big)F_j u_t\big\|\Big\}\right)^2}.$$

Step 2. *If $u_{t+1} = u_t$, then stop; otherwise, set $t := t + 1$ and return to* **Step 1.**

It is readily seen that, for the case where $n = 1 = m$, in the MSSFPMOS (1.2), accordingly in Algorithm 1, as an immediate consequence of Theorem 3.2, we obtain the following result which solves the SFP (1.1).

Corollary 3.4. *Assume that the set of solutions $\Pi = C \cap F^{-1}(Q)$ of the SFP (1.1) is non-empty and suppose that the sequences $\{\sigma_t\}$ and $\{\rho_t\}$ in Algorithm 3 satisfy the assumptions (a1) and (a2) in Theorem 3.2. Then, the sequence $\{u_t\}$ generated by Algorithm 3 converges*

strongly to an element $u^* \in \Pi$, *where* $u^* = P_\Pi 0$.

Algorithm 3: A self-adaptive approximation technique for SFP (1.1)

Step 0. *Choose two sequences* $\{\sigma_t\} \subset (0,1)$ *and* $\{\rho_t\} \subset (0,2)$ *and select* $\beta > 0$. *Let* $u_0 \in H_1$ *be arbitrary initial guess and set* $t := 0$.

Step 1. *Given the current iterate* u_t, *compute the next iterate* u_{t+1} *via the formula*

$$u_{t+1} = P_{C_t^2}\Big((1-\sigma_t)\big(u_t - \tau_t F^*\big(I - P_{Q_t^2}\big)Fu_t\big)\Big),$$

where $C_t^2 = C_t \cap C_{t-1}$, $Q_t^2 = Q_t \cap Q_{t-1}$, *and the stepsize* τ_t *is self-adaptively defined by*

$$\tau_t := \frac{\rho_t \big\|\big(I - P_{Q_t^2}\big)Fu_t\big\|^2}{\Big(max\big\{\beta,\ \big\|F^*\big(I - P_{Q_t^2}\big)Fu_t\big\|\big\}\Big)^2}.$$

Step 2. *If* $u_{t+1} = u_t$, *then stop; otherwise, set* $t := t+1$ *and return to* **Step 1.**

4. Numerical Experiments

In this section, we perform some computational tests to illustrate the implementation and efficiency of our proposed algorithm and we compare it with several existing methods in the literature.

The numerical results are completed on a standard TOSHIBA laptop with Intel(R) Core(TM) i5-2450M CPU@2.5GHz 2.5GHz with memory 4GB. The code is implemented in MATLAB R2020a.

Example 4.1. Let $H = \mathbb{R}^3$, $H_1 = \mathbb{R}^6$, $H_2 = \mathbb{R}^9$, $H_3 = \mathbb{R}^{12}$ and $H_4 = \mathbb{R}^{15}$. Find a point $u^* \in \mathbb{R}^3$ such that

$$u^* \in \Omega := C_1 \cap \Big(\cap_{j=1}^4 F_j^{-1}(Q_j)\Big) \neq \emptyset, \tag{4.1}$$

where

$$\begin{aligned} C_1 &= \{u \in \mathbb{R}^3 : \|u - o_1\|^2 \leq r_1^2\},\\ Q_1 &= \{F_1 u \in \mathbb{R}^6 : \|F_1 u - O_1\|^2 \leq R_1^2\},\\ Q_2 &= \{F_2 u \in \mathbb{R}^9 : \|F_2 u - O_2\|^2 \leq R_2^2\},\\ Q_3 &= \{F_3 u \in \mathbb{R}^{12} : \|F_3 u - O_3\|^2 \leq R_3^2\},\\ Q_4 &= \{F_4 u \in \mathbb{R}^{15} : \|F_4 u - O_4\|^2 \leq R_4^2\}, \end{aligned}$$

where o_1, $O_1 \in \mathbb{R}^6$, $O_2 \in \mathbb{R}^9$, $O_3 \in \mathbb{R}^{12}$, $O_4 \in \mathbb{R}^{15}$, $r_1, R_1, R_2, R_3, R_4 \in \mathbb{R}$, and $F_1 : \mathbb{R}^3 \to \mathbb{R}^6$, $F_2 : \mathbb{R}^3 \to \mathbb{R}^9$, $F_3 : \mathbb{R}^3 \to \mathbb{R}^{12}$, and $F_4 : \mathbb{R}^3 \to \mathbb{R}^{15}$.

For any $u \in \mathbb{R}^3$, we have $c_1(u) = \|u - o_1\|^2 - r_1^2$ and $q_j(F_j u) = \|F_j u - O_j\|^2 - R_j^2$ for $j = 1,2,3,4$. In what follows the subgradients ξ_1^t and η_j^t of respectively $c_1(u_t)$ and $q_j(F_j u_t)$ can be calculated respectively at the points u_t and $T_j u_t$ by $\xi_1^t(u_t) = 2(u_t - o_1)$ and $\eta_j^t(F_j u_t) = 2(F_j u_t - O_j)$. Thus, according to (3.2) and (3.3), the half-spaces C_1^t and Q_j^t $(j = 1,2,3,4)$, respectively of the sets C_1 and Q_j can be easily determined at a point u_t and $F_j u_t$, respectively, and the metric projections onto the half-paces C_1^2 and $Q_{j,t}^{int}$ $(j = 1,2,3,4)$, can be easily computed.

Now, we take, the radii $r_1 = 4$, $R_1 = 8$, $R_2 = 15$, $R_3 = 22$, $R_4 = 18$, the elements of the representing matrices F_j are randomly generated in the closed interval $[-5, 5]$, and the centers

$$o_1 = (0.4, 0.6, 0.6)^T, O_1 = (0.1, -0.5, 0.4, -0.5, -0.1, -0.2)^T,$$
$$O_2 = (0.1, 1.0, 0.5, 1.0, -0.5, 0.1, -0.9, 0.5, 0.2)^T,$$
$$O_3 = (0.7, 1.0, 0.9, -0.2, -1.0, 0.1, -0.6, -0.6, -0.3, -0.9, 0.5, 0.5)^T,$$
$$O_4 = (0.1, -0.3, 0.7, 0.1, 0.9, 0.8, -0.3, 0.1, -0.3, 0.26, 0.6, 0.5, -0.7, 0.6, -0.9)^T.$$

In example 4.1, we examine the convergence of the sequence $\{u_t\}$ generated by Algorithm 1 compared to the iterative methods given by Algorithm (3.30) and Algorithm (3.31). For this purpose, we consider the values of the parameters appeared in the methods as follows. We take $\beta = 0.3$, $\rho_t = \frac{t}{2t+1}$, $\sigma_t = \frac{1}{10t}$, $\alpha_1^t = 1$, $\beta_j = \frac{j}{10}$ $(j = 1, 2, 3, 4)$, $x_0 = (-1, 3, -2)^T$. Moreover, in Algorithms (3.30) and (3.31), we take $\tau_t = 0.0005$ and $f(u) = 0.975u$ in Algorithm (3.31).

In this experiment, we use $E_t = \|u_{t+1} - u_t\|^2 < \epsilon$ for small enough $\epsilon > 0$ as a stopping criteria. In Table 1 and Figure 1, we report the numerical results of the compared methods for different values of ϵ.

Table 1. Numerical results of compared methods for different values of ϵ.

		Algorithm 1	Algorithm (3.30)	Algorithm (3.31)
	Iter. (t)	23	27	41
$\epsilon = 10^{-4}$	cpu(s)	0.001590	0.016056	0.007037
	Iter. (t)	49	60	105
$\epsilon = 10^{-6}$	cpu(s)	0.001393	0.001567	0.001662
	Iter. (t)	72	115	168
$\epsilon = 10^{-8}$	cpu(s)	0.015945	0.011189	0.017034
	Iter. (t)	190	212	245
$\epsilon = 10^{-10}$	cpu(s)	0.032656	0.041615	0.062844

It is readily apparent from Table 1 and Figure 1 that Algorithm 1 exhibits superior performance compared to the other algorithms, as evidenced by its lower number of iterations and shorter runtime in seconds.

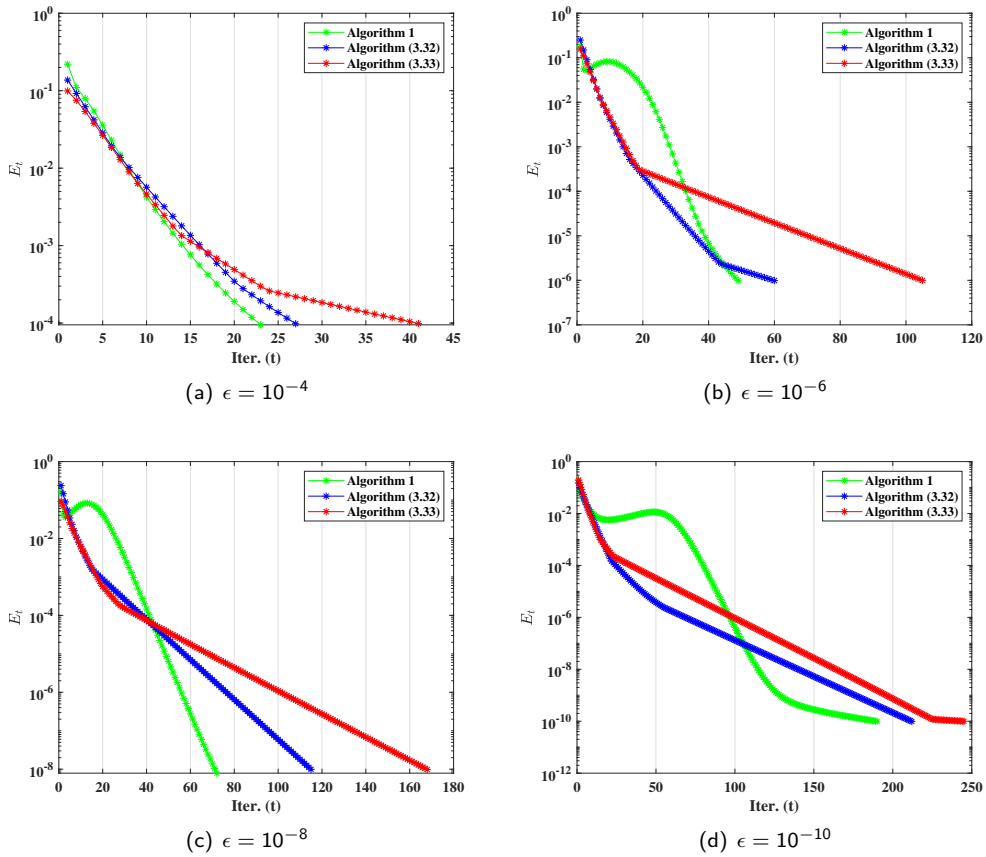

(a) $\epsilon = 10^{-4}$ (b) $\epsilon = 10^{-6}$

(c) $\epsilon = 10^{-8}$ (d) $\epsilon = 10^{-10}$

Fig. 1. Iter. (t) against Error, experimental results of compared methods for different values of ϵ.

Example 4.2. Let $H_1 = H_2 = L_2([0,1])$ with the inner product $\langle \cdot, \cdot \rangle$ and induced norm $\| \cdot \|$ defined by

$$\langle u, v \rangle = \int_0^1 u(s)v(s)ds, \ \forall u, v \in L_2([0,1]),$$

$$\|u\|_2 := \sqrt{\int_0^1 |u(s)|^2 ds}, \ \forall u \in L^2([0,1]).$$

Furthermore, we consider the following half-spaces

$$C := \left\{ u \in L^2([0,1]) : \langle u(s), 3s^2 \rangle = 0 \right\} \text{ and}$$

$$Q := \left\{ v \in L^2([0,1]) : \langle v, \frac{s}{3} \rangle \geq -1 \right\}.$$

In addition, we consider a linear continuous operator $F : L_2([0,1]) \to L_2([0,1])$, where

$(Fu)(s) = u(s)$. Then, $(F^*u)(s) = u(s)$ and $\|F\| = 1$. That is, F is an identity operator. The metric projection onto an half-space has an explicit formula [4]. Now, we solve the following problem

$$\text{find } u^* \in C \text{ such that } Fu^* \in Q. \tag{4.2}$$

In Example 4.2, we examine the numerical behaviour of our proposed method: Algorithm 3 and compare it with the following strongly convergent iterative algorithms, repesctively introduced by López et al. [14] and He et al. [13] by solving problem (4.2). For $u, u_0 \in H_1$;

$$u_{t+1} := \sigma_t u + (1-\sigma_t)P_{C_t}\Big(u_t - \tau_t F^*(I - P_{Q_t})Fu_t\Big), \forall t \geq 1, \tag{4.3}$$

$$u_{t+1} := P_{C_t}\Big(\sigma_t u + (1-\sigma_t)\big(u_t - \tau_t F^*(I - P_{Q_t})Fu_t\big)\Big), \tag{4.4}$$

where C_t and Q_t are given as in (1.6) and (1.7), respectively, $\{\sigma_t\} \subset (0,1)$, and $\tau_t = \frac{\rho_t\|(I-P_{Q_t})Fu_t\|^2}{\|F^*(I-P_{Q_t})Fu_t\|^2}$ with $\rho_t \subset (0,2)$.

For comparison purpose, we take the following data: In all methods, $\rho_t = \frac{t}{2t+1}$ and $\sigma_t = 0.5$. Moreover, we take $\beta = 0.3$ in Algorithm 3 and fix $u = cos(s)$ in Algorithms (4.3) and (4.4).

Now, using $E_t = \|u_{t+1} - u_t\| < 10^{-4}$ as stopping criteria for all methods, for different choices of the initial point u_0, the outcomes of the numerical experiments of the compared methods are reported in Table 2 and Figure 2.

Table 2. Comparison of Algorithm 3 with Algorithms (4.3) and (4.4) for different choices of u_0

		Algorithm 3	Algorithm (4.3)	Algorithm (4.4)
	Iter. (t)	18	21	20
$u_0 = s^3$	cpu(s)	0.178345	0.337353	0.468288
	Iter. (t)	18	20	20
$u_0 = s$	cpu(s)	0.176935	0.322715	0.458368
	Iter. (t)	17	21	20
$u_0 = se^s$	cpu(s)	0.164977	0.319452	0.446301
	Iter. (n)	18	20	20
$u_0 = sin(s)$	cpu(s)	0.165513	0.306389	0.447171

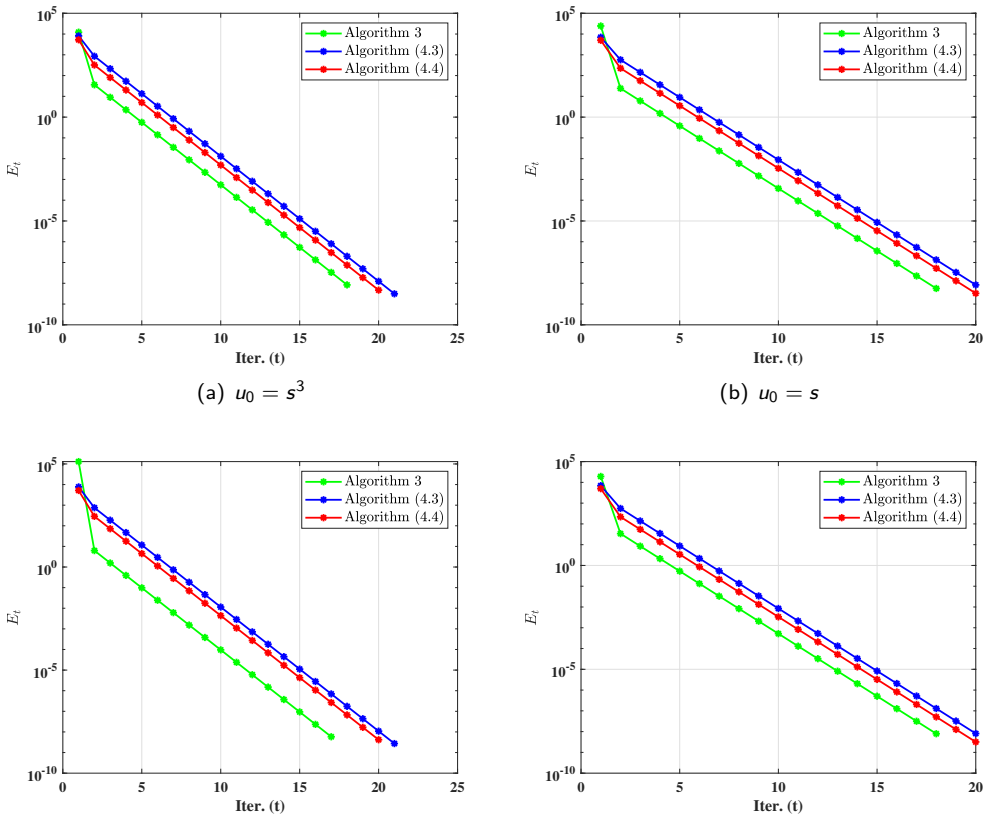

(a) $u_0 = s^3$ (b) $u_0 = s$

(c) $u_0 = se^s$ (d) $u_0 = sin(s)$

Fig. 2. Comparison of Algorithm 3 with Algorithms (4.3) and (4.4) for different choices of u_0

It can be observed from Table 2 and Figure 2 that for each choices of u_0, Algorithm 3 is faster in terms of less number of iterations (Iter. (t)) and cpu-run time in seconds (cpu(s)) than the compared algorithms.

Example 4.3. In this Example, we consider numerical experiments to illustrate the application of the proposed algorithm to inverse problems arising from signal processing. Compressed sensing is a very active domain of research and applications, based on the fact that an N-sample signal u with exactly K nonzero components can be recovered from $K \ll M < N$ measurements as long as the number of measurements is smaller than the number of signal samples and at the same time much larger than the sparsity level of u. Likewise, the measurements are required to be incoherent, which means that the information contained in the signal is spread out in the domain. Since $M < N$, the problem of recovering u from M measurements is ill conditioned because we encounter an underdeterminated system of linear equations. But, using a sparsity prior, it turns out that reconstructing u from b is possible as long as the number of nonzero elements is small enough (see [18]). More specifically, compressed sensing can be formulated as inverting the equation system

$$b = Fu + \Sigma, \tag{4.5}$$

where $u \in \mathbb{R}^N$ is a vector with K nonzero components to be recovered, $b \in \mathbb{R}^M$ is the vector of noisy observations or measurements (the measured data) with noisy Σ (when $\Sigma = 0$, it means that there is no noise to the observed data), and $F : \mathbb{R}^N \to \mathbb{R}^M$ is a bounded linear observation operator, often ill-conditioned because it models a process with loss of information. A powerful approach for problem (4.5) consists in considering a solution u represented by a sparse expansion, that is, represented by a series expansion with respect to an orthonormal basis that has only a small number of large coefficients. When attempting to find sparse solutions to linear inverse problems of type (4.5), successful model is the convex unconstrained minimization problem

$$\min_{u\in\mathbb{R}^N} \frac{1}{2}\|Fu - b\|_2^2 + \varrho\|u\|_1, \tag{4.6}$$

where ϱ is positive parameter and $\|.\|_1$ is the ℓ_1 norm. Problem (4.6) consists in minimizing an objective function, which includes a quadratic error term combined with a sparseness-including ℓ_1 regularization term, which is to make small component of u to become zero. Problem (4.5) can be seen as the following least absolute shrinkage and selection operator (LASSO), which is commonly used in the theory of signal processing (see [11])

$$\min_{u\in\mathbb{R}^N} \frac{1}{2}\|Fu - b\|_2^2 \text{ subject to } \|u\|_1 \leq \varpi, \tag{4.7}$$

where $\varpi > 0$ is a given constant. By the theory of convex analysis, one is able to show that a solution to the LASSO problem (4.7), for appropriate choices $\varpi > 0$, is a minimizer of (4.6) (see [9]). It can be observed that (4.7) indicates the potential of finding a sparse solution of the SFP (1.1) due to the ℓ_1 constraint. More precisely, it is readily seen that problem (4.7) is a particular case of the SFP (1.1) with $C := \{u : \|u\|_1 \leq \varpi\}$ and $Q = \{b\}$, and thus can be solved by Algorithm 3 and the iterative methods given by Algorithms (4.3) and (4.4). We define the convex function $c(u) = \|u\|_1 - \varpi$, and according (1.6), the level set C_t is defined by

$$C_t = \{u \in \mathbb{R}^N : c(u_t) + \langle \xi_t, u - u_t\rangle \leq 0\},$$

where $\xi_t \in \partial c(u_t)$. Observe that the metric projection onto C_t can be computed by the following manner,

$$P_{C_t}(v)) = \begin{cases} v, & \text{if} \quad c(u_t) + \langle \xi_t, v - u_t\rangle \leq 0, \\ v - \frac{\langle c(u_t) + \langle \xi_t, v - u_t\rangle}{\|\xi_t\|_{l^2}^2}\xi_t, & \text{otherwise.} \end{cases}$$

We choose a subgradient $\xi_t \in \partial c(u_t)$ as

$$(\xi_t)_i = \begin{cases} 1 & \text{if} \quad (\xi_t)_i > 0, \\ 0 & \text{if} \quad (\xi_t)_i = 0, \\ -1 & \text{if} \quad (\xi_t)_i < 0. \end{cases}$$

In a special case where $Q = Q_t = \{b\}$, Algorithm 3 converges to the solution of (4.7). Moreover, Algorithm 3 can be implemented easily, because the projection onto the level set

has an explicit formula. In order to show the efficiency of Algorithm 3, a comparative sparse signal recovery experiments were carried-out with Algorithms (4.3) and (4.4).

The vector u is a K sparse signal with non-zero K elements that are generated from uniform distribution within an interval of $[-2, 2]$, F is a matrix generated from normal distribution with mean zero and variance of one and b is an observation generated by white Gaussian noise with signal-to-noise ratio $SNR = 40$. The process of sparse signal recovery start by randomly generating $\varpi = K$ and the anchor (in Algorithms (4.3) and (4.4)) and initial point u_0 are $N \times 1$ vectors. The main target is then to recover the K sparse signal by solving (4.7) for u. The restoration accuracy is then measured by mean squared error (MSE) as follows:

$$MSE = \frac{\|u_{t+1} - u\|}{N} \leq \epsilon, \tag{4.8}$$

where u_t is an estimated signal of u, and $\epsilon > 0$ is a given small constant. We choose the parameters $\sigma_t = \frac{1}{10t+1}$, $\rho_t = 0.5$, $\beta = 0.3$. In our numerical experiments, for $u =$ ones $([N, 1])$ and $u_0 =$ ones $([N, 1])$, we consider the following four choices.

Data 1: $K = 20, N = 2^{14}, M = 2^{12}$;

Data 2: $K = 40, N = 2^{14}, M = 2^{12}$;

Data 3: $K = 20, N = 2^{16}, M = 2^{14}$;

Data 4: $K = 40, N = 2^{16}, M = 2^{14}$.

We use $MSE < \epsilon = 10^{-4}$ as stopping criterion for all methods. The results of the numerical experiments interms of number of iterations (Iter. (t)) and the cpu-run time in seconds (cpu(s)) are reported in Table 3 and Figures 3-6.

Table 3. The experiments of compressed sensing via Algorithm 3, Algorithm (4.3), and Algorithm (4.4)

	Algorithm 3			Algorithm (4.3)			Algorithm (4.4)		
	Iter. (t)	cpu(s)	MSE	Iter. (t)	cpu(s)	MSE	Iter. (t)	cpu(s)	MSE
Data 1	45	4.1563	9.8312e-05	77	7.2441	9.9181e-05	58	5.4076	9.8756e-05
Data 2	74	6.9091	9.8402e-05	96	9.0256	9.8874e-05	83	7.8555	9.6997e-05
Data 3	26	31.3975	9.4105e-05	43	53.1184	9.5889e-05	34	42.1191	9.9678e-05
Data 4	34	41.0025	9.7336e-05	52	63.3655	9.7688e-05	40	48.7032	9.9927e-05

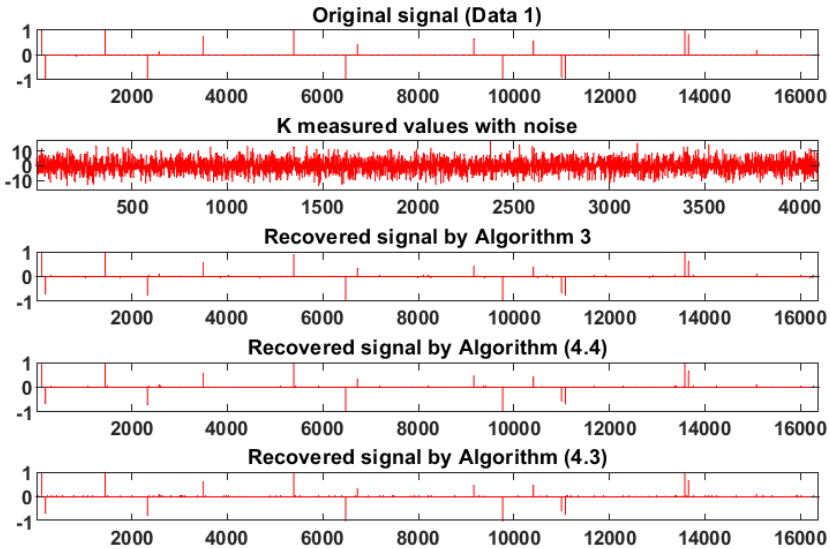

Fig. 3. Original K-sparse vs recovered sparse signals by compared methods for Data 1

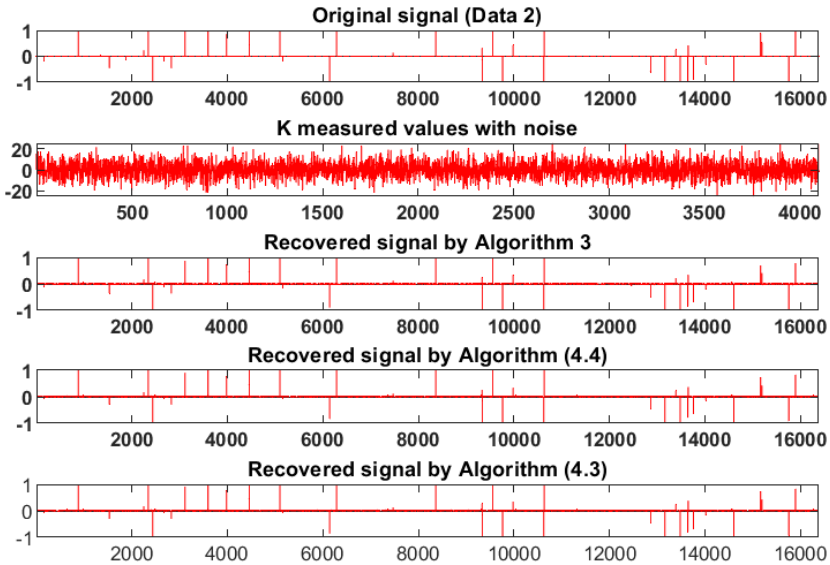

Fig. 4. Original K-sparse vs recovered sparse signals by compared methods for Data 2

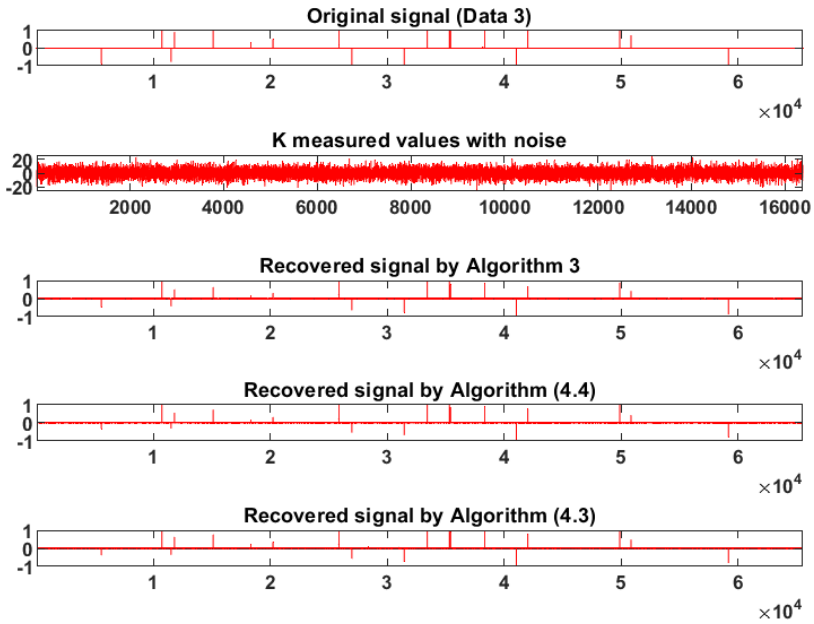

Fig. 5. Original K-sparse vs recovered sparse signals by compared methods for Data 3

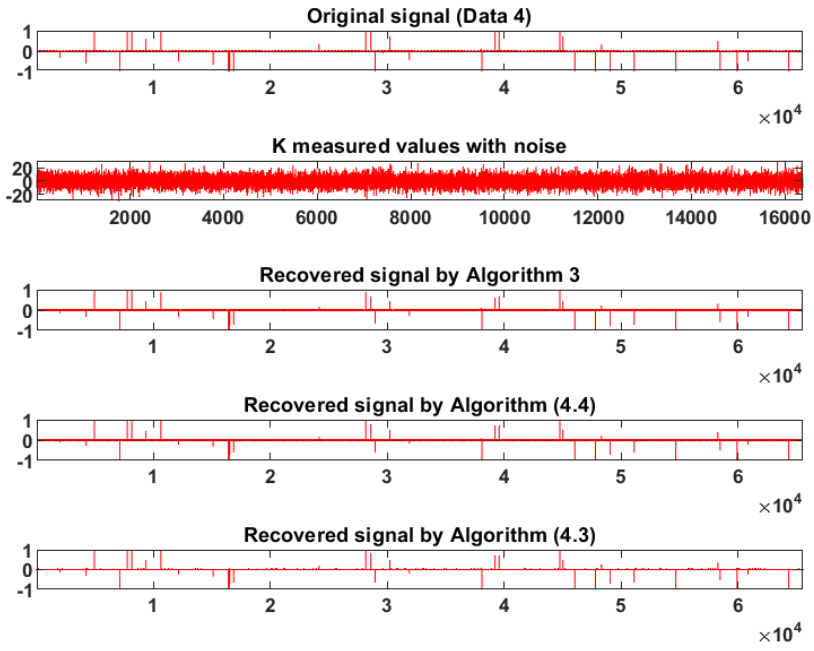

Fig. 6. Original K-sparse vs recovered sparse signals by compared methods for Data 4

It can be observed from Table 3 and Figures 3-6 that the recovered signal by the proposed method has less number of iterations and small cpu(s) time to converge than by the compared methods.

Competing interests

The authors declare that they have no competing interests.

Author's contributions

All authors contributed equally to the manuscript: checked, read, and approved the final manuscript.

Acknowledgments

This research project is supported by Thailand Science Research and Innovation (TSRI) Basic Research Fund: Fiscal year 2023 under project number FRB660073/0164. The authors also acknowledge the financial support provided by the Center of Excellence in Theoretical and Computational Science (TaCS-CoE), KMUTT. Moreover, Guash Haile Taddele would like to thank the Postdoctoral Fellowship from King Mongkut's University of Technology Thonburi (KMUTT), Thailand.

References

[1] H.H. Bauschke and P.L. Combettes, Convex analysis and monotone operator theory in Hilbert spaces, Springer, 2011.

[2] C. Byrne, Iterative oblique projection onto convex sets and the split feasibility problem, Inverse problems, 18 (2) (2002), 441.

[3] C. Byrne, A unified treatment of some iterative algorithms in signal processing and image reconstruction, Inverse problems, 20 (1) (2003), 103.

[4] A. Cegielski, Iterative methods for fixed point problems in Hilbert spaces, Springer, 2012.

[5] Y. Censor, A. Gibali and S. Reich, Algorithms for the split variational inequality problem, Numer. Algorithms., 59 (2) (2012), 301–323.

[6] Y. Censor and T. Elfving, A multiprojection algorithm using Bregman projections in a product space, Numer. Algorithms., 8 (2) (1994), 221–239.

[7] Y. Censor, T. Elfving , N. Kopf and T. Bortfeld, The multiple-sets split feasibility problem and its applications for inverse problems, Inverse Problems, 21 (6) (2005), 2071.

[8] Y. Dang and Y. Gao, The strong convergence of a KM–CQ-like algorithm for a split feasibility problem, Inverse Problems, 27 (1) (2010), 015007.

[9] M.A. Figueiredo, R.D. Nowak and S.J. Wright, Gradient projection for sparse reconstruction: Application to compressed sensing and other inverse problems, IEEE Journal of selected topics in signal processing, 1 (4) (2007), 586–597.

[10] M. Fukushima, A relaxed projection method for variational inequalities, Math Program, 35 (1) (1986), 58–70.

[11] A. Gibali, L.W. Liu and Y.C. Tang, Note on the modified relaxation CQ algorithm for the split feasibility problem, Optim. Lett., 12 (4) (2018), 817–830.

[12] S. He and C. Yang, Solving the variational inequality problem defined on intersection of finite level sets, In: Abstract and Applied Analysis, vol. 2013, Hindawi, 2013.

[13] S. He and Z. Zhao, Strong convergence of a relaxed CQ algorithm for the split feasibility problem, J. Inequal. Appl., 2013 (1) (2013), 197.

[14] G. López, V. Martín-Márquez, F. Wang and H.K. Xu, Solving the split feasibility problem without prior knowledge of matrix norms, Inverse Problems, 28 (8) (2012), 085004.

[15] G. López, V. Martin and H. Xu, Iterative algorithms for the multiple-sets split feasibility problem, Biomedical mathematics: promising directions in imaging, therapy planning and inverse problems, (2009), 243–279.

[16] P.E. Maingé, A hybrid extragradient-viscosity method for monotone operators and fixed point problems, SIAM J. Control Optim., 47 (3) (2008), 1499–1515.

[17] S. Reich, M.T. Truong and T.N.H. Mai, The split feasibility problem with multiple output sets in Hilbert spaces, Optim. Lett., (2020), 1–19.

[18] J.L. Starck, F. Murtagh and J.M. Fadili, Sparse image and signal processing: wavelets, curvelets, morphological diversity, Cambridge University Press, 2010.

[19] T. Suzuki, A sufficient and necessary condition for Halpern-type strong convergence to fixed points of nonexpansive mappings, Proc. Amer. Math. Soc. Ser., 135 (1) (2007), 99–106.

[20] F. Wang and H.K. Xu, Approximating curve and strong convergence of the CQ algorithm for the split feasibility problem, J. Inequal. Appl., 2010 (2010), 1–13.

[21] H.K. Xu, Iterative algorithms for nonlinear operators, J. Lond. Math. Soc., 66 (1) (2002), 240–256.

[22] H.K. Xu, A variable Krasnosel'skii–Mann algorithm and the multiple-set split feasibility problem, Inverse problems, 22 (6) (2006), 2021.

[23] H.K. Xu, Iterative methods for the split feasibility problem in infinite-dimensional Hilbert spaces, Inverse Problems, 26 (10) (2010),105018.

[24] Q. Yang, The relaxed CQ algorithm solving the split feasibility problem, Inverse problems, 20 (4) (2004), 1261.

[25] Q. Yang, On variable-step relaxed projection algorithm for variational inequalities, J. Math. Anal. Appl., 302 (1) (2005), 166–179.

[26] Q. Yang and J. Zhao, Generalized KM theorems and their applications, Inverse Problems, 22 (3) (2006), 833.

[27] X. Yu, N. Shahzad and Y. Yao, Implicit and explicit algorithms for solving the split feasibility problem, Optim. Lett., 6 (7) (2012), 1447–1462.

[28] H. Yu and F. Wang, A new relaxed method for the split feasibility problem in Hilbert spaces, Optimization, (2022), 1–16.

[29] H. Yu, W. Zhan and F. Wang, The ball-relaxed CQ algorithms for the split feasibility problem, Optimization, 67 (10) (2018),1687–1699.

[30] J. Zhao and Q. Yang, Self-adaptive projection methods for the multiple-sets split feasibility problem, Inverse Problems, 27 (3) (2011), 035009.

Nonlinear Convex Analysis and Optimization
Vol. 2, No. 1, 2023, pp. 31–53
https://ncao.design.blog

Fermatean Fuzzy Divergences and Their Applications to Decision-making and Pattern Recognition

Wiyada Kumam[a,1,*], Konrawut Khammahawong[a,2], Muhammad Jabir Khan[b,3], Thanatporn Bantaojai[c,4], Supak Phiangsungnoen[d,5]

[a]Lecturer, Applied Mathematics for Science and Engineering Research Unit (AMSERU), Program in Applied Statistics, Department of Mathematics and Computer Science, Faculty of Science and Technology, Rajamangala University of Technology Thanyaburi (RMUTT), Pathum Thani 12110, Thailand
[b]Researcher, Center of Excellence in Theoretical and Computational Science (TaCS-CoE), SCL 802 Fixed Point Laboratory, Science Laboratory Building, King Mongkut's University of Technology Thonburi (KMUTT), 126 Pracha-Uthit Road, Bang Mod, Thung Khru, Bangkok 10140, Thailand
[c]Mathematics (English Program), Faculty of Education, Valaya Alongkorn Rajabhat University under the Royal Patronage, Pathum Thani 13160, Thailand
[d]General Education (Mathematics Program), Faculty of Liberal Arts, Rajamangala University of Technology Rattanakosin, Samphanthawong, Bangkok 10100, Thailand
[1]wiyada.kum@rmutt.ac.th; [2]konrawut_k@rmutt.ac.th; [3]jabirkhan.uos@gmail.com;
[4]thanatporn.ban@vru.ac.th; [5]supak.pia@rmutr.ac.th
* Corresponding Author

ABSTRACT

Fermatean fuzzy sets (FFS) generalized the Intuitionistic fuzzy set and Pythagorean fuzzy set in terms of more space available to choose orthopairs. The manuscript provides Chi-square and Canberra divergence measures for FFSs. Divergence measurements' additional characteristics are looked into to ensure good performance. The entropy and dissimilarity measures from the suggested divergence measures are derived. A technique is developed to transform the real or fuzzy data into Fermatean fuzzy data. An empirically successful VIKOR method is extended for FFSs. The Australasian New Car Assessment Program (ANCAP) provides the star rankings from a safety point of view for each vehicle. The VIKOR method is employed to draw safety rankings of small cars tested from 2019 to 2021 by ANCAP. The numerical examples are given to clarify each method under discussion.

Article History
Received 12 Feb 2023
Revised 8 April 2023
Accepted 25 May 2023
Keywords:
Fermatean fuzzy sets;
Decision making;
Divergence measures;
VIKOR method;
Fuzzification technique
MSC
53C 05

1. Introduction

The notion of fuzzy sets was developed as a way to mathematically represent the ambiguity we often use to explain events that don't have clearly defined boundaries. The number of

Please cite this article as: W. Kumam et al., Fermatean Fuzzy Divergences and Their Applications to Decision-making and Pattern Recognition, Nonlinear Convex Anal. & Optim., Vol. 2 No. 1, 31–53. https://doi.org/10.58715/ncao.2023.2.2

items encountered in human reasoning that can be the subject of scientific research is enlarged by employing the idea of partial degrees of membership to create a mathematical description of fuzzy sets [30]. However, The negative side of information is required in real-life scenarios and cannot only be retrieved from the positive side. For instance, the use of antibiotic medications, while beneficial in the treatment of various diseases, has some adverse effects on the body. Information's positive and negative aspects can be viewed as membership degree (MD) and non-membership degree (non-MD), respectively. A non-MD is distinct from a MD. In particular, Atanassov pioneered the idea of taking into account both MD and non-MDs and gave it the name intuitionistic fuzzy set (IFS) [2]. Figure 1 provides the geometric explanation of an IFS. In Figure 1, $(1,0)$ and $(0,1)$ symbolize absolute agreement and total disagreement, respectively, whereas $(0,0)$ denotes utter obscurity or ignorance of the situation. The triangular region's ordered pair $(\mu(u), \nu(u))$, also known as intuitionistic fuzzy value (IFV), indicates that the individual is μ percent agrees with the circumstance u and ν percent disagrees with it.

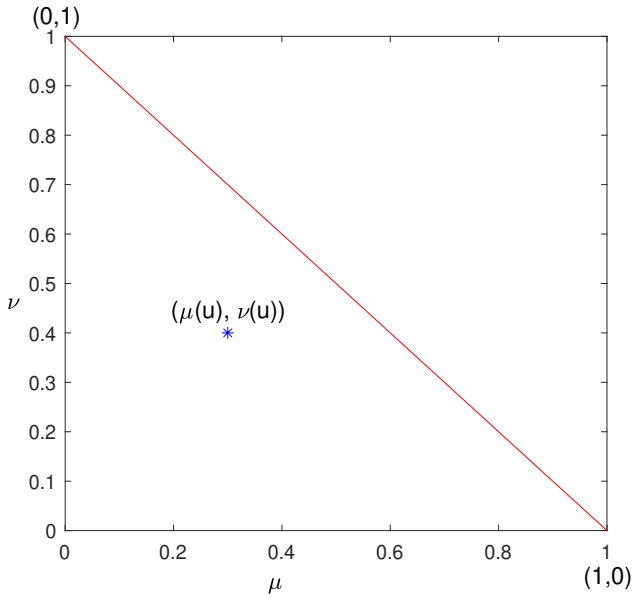

Fig. 1. Geometrical exposition of an IFS

The constraint on membership and non-membership may limit the applicability of IFS, despite the fact that it has been used to solve a variety of issues. This problem is somehow addressed by the introduction of Pythagorean fuzzy sets (PFSs) by Yager [28]. It relaxed the defining conditions, where sum of membership and no-MDs should be less than or equal to one. Recently, Senapati and Yager [27] extended the idea of IFS and PFS to Fermatean fuzzy sets (FFS). FFSs provides the larger space to choose orthopairs. In FFSs, the sum of cube of membership and non-MDs should be less than or equal to one. Figure 2 shows the geometrical interpretations of PFSs and FFSs. A clear picture of expanding the space for orthopairs for FFSs can be seen in Figure 2.

As it provides the larger space to choose orthopairs for membership and non-membership

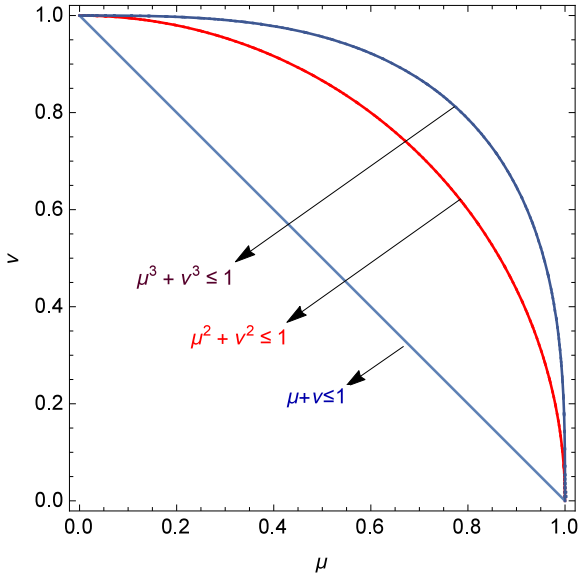

Fig. 2. The geometrical expositions and a comparison between the spaces available for IFS, PFS, and FFS

grades, many scholars have worked on its applications. The Fermatean fuzzy weighted average and geometric aggregation operators were established by Senapati and Yager [25]. They also discussed subtraction, arithmetic mean, and division operations for FFSs [26]. Garg et al. [7] developed different aggregation operators for FFSs and applied them to Covid-19 testing facility. Ghorabaee et al. [13] extended WASPAS for FFSs and discussed their applications to green supplier evaluation. Fermatean fuzzy Einstein aggregation operators and their applications were discuused by Akram et al. [1]. Liu et al. [17] introduced Fermatean fuzzy linguistic term set and their aggregation operators. MULTIMOORA method based on Fermatean fuzzy Einstein aggregation operators was discuused by Rani and Mishra [21]. The interval-valued FFSs and their basic properties were established by Jeevaraj [11]. Sahoo [24] provided new score function for FFSs and discussed fuzzy transportation problems. Fermatean fuzzy SAW, ARAS, and VIKOR method extensions were focused by Gul [8]. The MCDM method was developed based on Dempster–Shafer theory and entropy measure for FFSs [5]. Fermatean fuzzy Hamacher aggregation operators were established by Hadi et al. [9]. Aydemir discussed TOPSIS method using dombi aggregation operators for FFSs [3]. CRITIC-EDAS method for FFS and their applications to sustainable third-party reverse logistics providers were discussed by Mishra et al. [18].

Divergence measures were first proposed in classical probability spaces as a way to compare two probability distributions. The expression to estimate the difference between two fuzzy sets was developed by Bhandari et al. [4]. They suggested the non-negativity, symmetry, and identity of indiscernibles properties for the formula for divergences. Montes et al. [19] later presented an axiomatic definition for fuzzy divergence. Divergence measures play a significant role and are used in a variety of contexts, including image processing, image thresholding, decision-making, edge detection, pattern recognition, clustering, figure skating, et cetera [4,

19, 20, 15]. Zhou et al. [31] established the divergence metrics for the PFS based on the belief function. By using the divergence metric dependent VIKOR approach in a PF domain, renewable energy technologies were evaluated [22]. The axiomatically supported divergence measurements for the q-rung orthopair fuzzy environment were proposed by Khan et al. [14]. Riaz et al. [23] talked about correlation coefficients and how they are used in pattern analysis and clustering. Khan et al. [16] gave the theoretical justifications for the VIKOR method's successful empirical use.

The Australasian New Car Assessment Program (ANCAP) provides the safety ratings for each vehicle in a particular category. ANCAP is an Australasian-based independent vehicle safety authority established in 1993 and issues safety ratings for thousands of new vehicle makes models and variants. It provides relative safety ratings between vehicles of similar size. ANCAP safety ratings are helpful for occupants and pedestrians to avoid or minimize the effects of a crash. Although these ratings are valuable, ANCAP has not provided any specific rankings of vehicles. An interested buyer of a vehicle has many options, if he follow NCAP Safety Ratings. There are many vehicles with maximum (five) stars ratings. Therefore, it is hard for a person to choose a specific vehicle based on ANCAP Safety Ratings. Therefore, a method or technique is required to draw the rankings of vehicles that occurred in the same category. It will surely be helpful for the buyers. For more details, we refer to Section 5.2.

The motivations behind the extensions of fuzzy set theory are to provide the mechanism to deal with the uncertainty that transpires in real-life problems. Due to it, the fuzzification of the real data is of paramount importance. There exist many techniques to fuzzify real-life data. But there does not exist any approach for obtaining the data in Fermatean fuzzy form. Thus we provide a new appproach to transform the data into Fermatean fuzzy form. We are also driven to develop additional functions that extend the VIKOR technique for FFSs while respecting the axiomatic assumptions of divergence measures. The manuscript discusses the fuzziness and dissimilarity measures for FFSs. Lastly, we are motivated to provide the safety rankings to small cars tested by ANCAP during 2019 to 2021.

With that in mind, the purpose of this article is to describe novel divergence functions, uncertainty (entropy), and dissimilarity measurements for FFSs. And to provide a method of transformation of real or fuzzy data into Fermatean fuzzy form. Also, to continue the VIKOR approach for FFSs and to produce the safety rankings for small cars tested by ANCAP from 2019 to 2021.

The manuscript's key contributions are:

- We suggest Canberra divergence and generalized Chi-square measures for FFSs. We establish these measurements' axiomatic validity.
- We examine the extra characteristics of these systems that support mathematical reasoning.
- We talk about the measurements of entropy and dissimilarity for FFSs.
- We present a technique to transform real or fuzzy data into Fermatean fuzzy data.
- The study provides the safety rankings of small cars tested from 2019 to 2021 by ANCAP.
- The manuscript develops the FFSs VIKOR technique.
- This paper gives examples to illustrate our suggested approach.

The remainder of the article is structured as follows: Section 2 covers the fundamentals of FFSs. Section 3 proposes the new divergence measurements and their additional features for FFSs. In Sections 3.1 and 3.2, respectively, it is discussed how divergence metrics transform into entropy and dissimilarity measures. The process of converting real data into Fermatean fuzzy data is explained in Section 4. In Section 5.1, the divergence measure-based VIKOR approach for FFSs is suggested. Section 5.2, it is detailing how the suggested VIKOR approach can be used to rank the safety of small cars that have undergone ANCAP testing. The manuscript's concluding observations are included in Section 7.

2. Preliminaries

The fundamental definitions of FFSs are included in this section. There is mention of the fundamental functions of FFSs. Throughout the entire manuscript, U is a finite non-empty set called the universal set. Besides, the unit interval $[0,1]$ is represented by $\mathbf{I}$.

Definition 2.1. [2] An IFS A over a universal set U is defined as

$$A = \{(u, \mu_P(u), \nu_P(u)) \mid u \in U\},$$

where $\mu_A : U \to \mathbf{I}$ and $\nu_A : U \to \mathbf{I}$, with the constraint $\mu_A(u) + \nu_A(u) \leq 1$, are the MDs and non-MDs, respectively. The expression $\pi_A(u) = 1 - (\mu_A(u) + \nu_A(u))$ gives the hesitancy degree of an element $u \in U$.

3. Divergence Measures for FFSs

This section provides the axiomatic definition of FFSs' divergence measures. It investigates several functions that are consistent with the axioms underlying the FF divergence measure. We discuss the additional attributes of the suggested divergence measures and place special emphasis on the entropy and dissimilarity measures for FFSs.

Definition 3.1. If a function $Div : C(U) \times C(U) \to \Re$ satisfies the following axioms, it is referred to as a divergence measure for FFSs: for each $A_1, A_2, A_3 \in C(U)$,

(D1) $Div(A_1, A_2) = Div(A_2, A_1)$.

(D2) $Div(A_1, A_2) = 0 \iff A_1 = A_2$.

(D3) $Div(A_1 \cup A_3, A_2 \cup A_3) \leq Div(A_1, A_2)$.

(D4) $Div(A_1 \cap A_3, A_2 \cap A_3) \leq Div(A_1, A_2)$.

Unless otherwise stated, in this section $A_1 = \{(u_i, \mu_{A_1}(u_i), \nu_{A_1}(u_i)) \mid i = 1, \ldots, n\}$ and $A_2 = \{(u_i, \mu_{A_2}(u_i), \nu_{A_2}(u_i)) \mid i = 1, \ldots, n\}$ designate FFSs on the same set $U = \{u_1, \ldots, u_n\}$.

Definition 3.2. The interpretation of the divergence functions based on chi-square distances for FFSs is

$$\bar{D}_1(A_1, A_2) = \frac{1}{n} \sum_{i=1}^{n} \left[\frac{\left(\mu_{A_1}^{\beta}(u_i) - \mu_{A_2}^{\beta}(u_i)\right)^2}{\lambda + \mu_{A_1}^{\beta}(u_i) + \mu_{A_2}^{\beta}(u_i)} + \frac{\left(\nu_{A_1}^{\beta}(u_i) - \nu_{A_2}^{\beta}(u_i)\right)^2}{\lambda + \nu_{A_1}^{\beta}(u_i) + \nu_{A_2}^{\beta}(u_i)} \right], \tag{3.1}$$

where $\lambda > 0$ and $1 \leq \beta \leq 3$.

Remark 3.3. The values of the parameters λ and β chosen empirically. For other values, the function still remain the divergence measure for FFSs. It is better to take the minimum value for λ.

Theorem 3.4. *The mapping $\bar{D}_1 : C(U)\times C(U) \to \Re$ described in (3.1) satisfies the divergence measure axioms.*

Proof. We must confirm the divergence axioms for $\bar{D}_1$ to finish the proof.

- (D1-D2) Straightforward.
- (D3) For any FFSs $A_1 = (\mu_{A_1}, \nu_{A_1})$, $A_2 = (\mu_{A_2}, \nu_{A_2})$ and $A_3 = (\mu_{A_3}, \nu_{A_3})$, the mapping $\bar{D}_1$ requires to fulfill

$$\bar{D}_1(A_1 \cap A_3, A_2 \cap A_3) \leq \bar{D}_1(A_1, A_2). \tag{3.2}$$

Now,

$$\bar{D}_1(A_1 \cap A_3, A_2 \cap A_3) = \frac{1}{n}\sum_{i=1}^{n}\left[\frac{\left((\min\{\mu_{A_1}, \mu_{A_3}\})^{\beta} - (\min\{\mu_{A_2}, \mu_{A_3}\})^{\beta}\right)^2}{\lambda + (\min\{\mu_{A_1}, \mu_{A_3}\})^{\beta} + (\min\{\mu_{A_2}, \mu_{A_3}\})^{\beta}}\right.$$
$$\left. + \frac{\left((\max\{\nu_{A_1}, \nu_{A_3}\})^{\beta} - (\max\{\nu_{A_2}, \nu_{A_3}\})^{\beta}\right)^2}{\lambda + (\max\{\nu_{A_1}, \nu_{A_3}\})^{\beta} + (\max\{\nu_{A_2}, \nu_{A_3}\})^{\beta}}\right]. \tag{3.3}$$

From $\min\{\mu_{A_1}, \mu_{A_3}\}$, $\min\{\mu_{A_2}, \mu_{A_3}\}$, $\max\{\nu_{A_1}, \nu_{A_3}\}$, and $\max\{\nu_{A_2}, \nu_{A_3}\}$, the following results are deduced,

$$\mu_{A_1} \leq \mu_{A_3} \leq \mu_{A_2} \quad or \quad \mu_{A_2} \leq \mu_{A_3} \leq \mu_{A_1} \quad or \tag{3.4}$$
$$\mu_{A_3} \leq \{\mu_{A_1} \& \mu_{A_2}\} \quad or \quad \mu_{A_3} \geq \{\mu_{A_1} \& \mu_{A_2}\} \quad \& \tag{3.5}$$
$$\nu_{A_1} \leq \nu_{A_3} \leq \nu_{A_2} \quad or \quad \nu_{A_2} \leq \nu_{A_3} \leq \nu_{A_1} \quad or \tag{3.6}$$
$$\nu_{A_3} \leq \{\nu_{A_1} \& \nu_{A_2}\} \quad or \quad \nu_{A_3} \geq \{\nu_{A_1} \& \nu_{A_2}\}. \tag{3.7}$$

The proof becomes straightforward for the inequalities in (3.5) and (3.7). We prove the results for (3.4) and (3.6). If $\mu_{A_1} \leq \mu_{A_3} \leq \mu_{A_2}$ and $\nu_{A_2} \leq \nu_{A_3} \leq \nu_{A_1}$, then (3.3) becomes

$$\bar{D}_1(A_1 \cap A_3, A_2 \cap A_3) = \frac{1}{n}\sum_{i=1}^{n}\left[\frac{\left(\mu_{A_1}^{\beta} - \mu_{A_3}^{\beta}\right)^2}{\lambda + \mu_{A_1}^{\beta} + \mu_{A_3}^{\beta}} + \frac{\left(\nu_{A_1}^{\beta} - \nu_{A_3}^{\beta}\right)^2}{\lambda + \nu_{A_1}^{\beta} + \nu_{A_3}^{\beta}}\right].$$

The divergence between the two FFSs A_1 and A_2 is

$$\bar{D}_1(A_1, A_2) = \frac{1}{n}\sum_{i=1}^{n}\left[\frac{\left(\mu_{A_1}^{\beta} - \mu_{A_2}^{\beta}\right)^2}{\lambda + \mu_{A_1}^{\beta} + \mu_{A_2}^{\beta}} + \frac{\left(\nu_{A_1}^{\beta} - \nu_{A_2}^{\beta}\right)^2}{\lambda + \nu_{A_1}^{\beta} + \nu_{A_2}^{\beta}}\right].$$

Since $\beta \geq 1$, therefore, $\mu_{A_1}^{\beta} \geq \mu_{A_3}^{\beta} \geq \mu_{A_2}^{\beta}$ and $\nu_{A_2}^{\beta} \geq \nu_{A_3}^{\beta} \geq \nu_{A_1}^{\beta}$, we have

$$\frac{\left(\mu_{A_1}^{\beta} - \mu_{A_3}^{\beta}\right)^2}{\lambda + \mu_{A_1}^{\beta} + \mu_{A_3}^{\beta}} \leq \frac{\left(\mu_{A_1}^{\beta} - \mu_{A_2}^{\beta}\right)^2}{\lambda + \mu_{A_1}^{\beta} + \mu_{A_2}^{\beta}} \quad \& \quad \frac{\left(\nu_{A_1}^{\beta} - \nu_{A_3}^{\beta}\right)^2}{\lambda + \nu_{A_1}^{\beta} + \nu_{A_3}^{\beta}} \leq \frac{\left(\nu_{A_1}^{\beta} - \nu_{A_2}^{\beta}\right)^2}{\lambda + \nu_{A_1}^{\beta} + \nu_{A_2}^{\beta}}.$$

This implies

$$\bar{D}_1(A_1 \cap A_3, A_2 \cap A_3) \leq \bar{D}_1(A_1, A_2).$$

We can similarly confirm the remaining parts of axiom (D3).

- (D4) Similar to the evidence of (D3).

The metric $\bar{D}_1$ is a divergence metric for FFSs as a result. It is simple to prove the evidence for $U = \{u_1, u_2, \ldots, u_n\}$. ∎

Definition 3.5. The interpretation of divergence functions based on the Canberra distances for FFSs is

$$\bar{D}_2(A_1, A_2) = \frac{1}{n}\sum_{i=1}^{n}\left[\frac{|\,\mu_{A_1}^{\beta}(u_i) - \mu_{A_2}^{\beta}(u_i)\,|}{\lambda + \mu_{A_1}^{\beta}(u_i) + \mu_{A_2}^{\beta}(u_i)} + \frac{|\,\nu_{A_1}^{\beta}(u_i) - \nu_{A_2}^{\beta}(u_i)\,|}{\lambda + \nu_{A_1}^{\beta}(u_i) + \nu_{A_2}^{\beta}(u_i)}\right], \tag{3.8}$$

where $\lambda > 0$ and $1 \leq \beta \leq 3$.

Theorem 3.6. *The expression $\bar{D}_2 : C(U) \times C(U) \to \Re$ described in (3.8) satisfies the divergence axioms.*

Proof. The evidence resembles the evidence of Theorem 3.4. ∎

There are further properties that the chi-square and Canberra divergence measures meet to ensure acceptable theoretical performance. They are shown in the following result.

Theorem 3.7. *The following properties are true for the divergence measures $\bar{D}_k$ $(k = 1, 2)$: If A_1, A_2 and A_3 be three FFSs, then*

T1. *For $\lambda = 1$, $\bar{D}_k(A_1, A_1^c) = 1$ if and only if either $\mu_{A_1} = 1$ or $\nu_{A_1} = 1$.*
T2. $\bar{D}_k(A_1^c, A_2) = \bar{D}_k(A_1, A_2^c)$.
T3. $\bar{D}_k(A_1, A_2) = \bar{D}_k(A_1^c, A_2^c)$.
T4. $\bar{D}_k(A_1 \cup A_2, A_1 \cap A_2) = \bar{D}_k(A_1, A_2)$.
T5. $\bar{D}_k(A_1 \cup A_2, A_3) \leq \bar{D}_k(A_1, A_3) + \bar{D}_k(A_2, A_3)$.
T6. $\bar{D}_k(A_1 \cap A_2, A_3) \leq \bar{D}_k(A_1, A_3) + \bar{D}_k(A_2, A_3)$.
T7. *Whenever $A_1 \subseteq A_2 \subseteq A_3$, we have $\bar{D}_k(A_1, A_3) \geq \max\{\bar{D}_k(A_1, A_2), \bar{D}_k(A_2, A_3)\}$.*

Proof. Suppose $A_1 = (\mu_{A_1}, \nu_{A_1})$, $A_2 = (\mu_{A_2}, \nu_{A_2})$ and $A_3 = (\mu_{A_3}, \nu_{A_3})$ to be three FFSs. Since $\bar{D}_1$ and $\bar{D}_2$ includes the factors $\triangle\mu_{12} = \mu_{A_1}^{\beta} - \mu_{A_2}^{\beta}$ and $\triangle\nu_{12} = \nu_{A_1}^{\beta} - \nu_{A_2}^{\beta}$. These variables form the basis of the divergence measures. With the aid of these elements, we prove the claims (**T1**-**T7**). If the related factors are identical on both sides, the proof will be considered conclusive.

T1: If $P = (\mu_P, \nu_P)$, then $P^c = (\nu_P, \mu_P)$. The metric $\bar{D}_1$ becomes

$$\bar{D}_1(P, P^c) = \frac{2\left(\mu_P^{\beta} - \nu_P^{\beta}\right)^2}{1 + \mu_P^{\beta} + \nu_P^{\beta}}. \tag{3.9}$$

Equation (3.9) becomes one only if either $\mu_A = 1$ or $\nu_A = 1$.
T2: For $A_1 = (\mu_{A_1}, \nu_{A_1})$ and $A_2 = (\mu_{A_2}, \nu_{A_2})$, their complements become $A_1^c = (\nu_{A_1}, \mu_{A_1})$ and $A_2^c = (\nu_{A_2}, \mu_{A_2})$. The measure $\bar{D}_1(A_1^c, A_2)$ contains $\triangle u_{12} = \nu_{A_1}^{\beta} - \mu_{A_2}^{\beta}$ and $\triangle v_{12} = \mu_{A_1}^{\beta} - \nu_{A_2}^{\beta}$. Also, the measure $\bar{D}_1(A_1, A_2^c)$ includes $\triangle u_{12}^{\star} = \mu_{A_1}^{\beta} - \nu_{A_2}^{\beta}$ and $\triangle v_{12}^{\star} = \nu_{A_1}^{\beta} - \mu_{A_2}^{\beta}$. It indicates that identical elements are present on both sides, guaranteeing that both sides are equal.
T3: Similar to the evidence from the earlier part.
T4: The side $\bar{D}_1(A_1 \cup A_2, A_1 \cap A_2)$ comprises of the following factors $\triangle u_{12} = (\max\{\mu_{A_1}, \mu_{A_2}\})^{\beta} - (\min\{\mu_{A_1}, \mu_{A_2}\})^{\beta}$, and $\triangle v_{12} = (\min\{\nu_{A_1}, \nu_{A_2}\})^{\beta} - (\max\{\nu_{A_1}, \nu_{A_2}\})^{\beta}$. While $\bar{D}_1(A_1, A_2)$ involves $\triangle u_{12}^{\star} = \mu_{A_1}^{\beta} - \mu_{A_2}^{\beta}$ and $\triangle v_{12}^{\star} = \nu_{A_1}^{\beta} - \nu_{A_2}^{\beta}$. It implies that $\mid \triangle u_{12} \mid = \mid \triangle u_{12}^{\star} \mid$ and $\mid \triangle v_{12} \mid = \mid \triangle v_{12}^{\star} \mid$, which guarantees that both sides are equal.
T5-T6: Straightforward.
T7: Similar to the Theorem 3.4 proof. ∎

3.1. Entropy Measure for FFSs

We present the divergence-based entropy metrics for FFSs in this section.

Definition 3.8. According to the divergence measures $\bar{D}_1$ and $\bar{D}_2$, the entropy measures of an FFS are as follows: for each $A \in C(U)$,

$$\bar{E}_k(A) = 1 - \frac{1}{F_k}\bar{D}_k(A, A^c), \tag{3.10}$$

where F_k is the constant function used to normalize the values and $\bar{D}_k(P, P^c)$ are

$$\bar{D}_1(A, A^c) = \frac{2}{n}\sum_{i=1}^{n}\left[\frac{\left(\mu_A^{\beta}(u_i) - \nu_A^{\beta}(u_i)\right)^2}{\lambda + \mu_A^{\beta}(u_i) + \nu_A^{\beta}(u_i)}\right],$$

$$\bar{D}_2(A, A^c) = \frac{2}{n}\sum_{i=1}^{n}\left[\frac{\mid \mu_A^{\beta}(u_i) - \nu_A^{\beta}(u_i) \mid}{\lambda + \mu_A^{\beta}(u_i) + \nu_A^{\beta}(u_i)}\right].$$

The key assertion of this section is stated in the result that follows.

Theorem 3.9. *The function $\bar{E}_k : C(U) \to [0, 1]$ expounded in (3.10) is an entropy measure.*

Proof. Straightforward. ∎

3.2. Dissimilarity Measure for IFSs

The research that has already been done on intuitionistic fuzzy divergences attests to the fact that they are the proper subset of the IF dissimilarity measures [20]. We do, however, confirm that the outcome holds true for FFSs. In other words, the axioms of dissimilarity measures are satisfied by the divergence measures $\bar{D}_1$ and $\bar{D}_2$.

Definition 3.10. If a mapping $Diss : C(U) \times C(U) \to \Re$ abides by the following axioms, it is referred to as a dissimilarity measure for FFSs: for each $A_1, A_2, A_3 \in C(U)$,

(D1) $Diss(A_1, A_2) = Diss(A_2, A_1)$.

(D2) $Diss(A_1, A_2) = 0 \Longleftrightarrow A_1 = A_2$.

(D3) Whenever $A_1 \subseteq A_2 \subseteq A_3$, we have $\bar{D}_k(A_1, A_3) \geq \max\{\bar{D}_k(A_1, A_2), \bar{D}_k(A_2, A_3)\}$.

Theorem 3.11. *The mappings $\bar{D}_1 \& \bar{D}_2 : C(U) \times C(U) \to \mathbf{I}$ abides the axioms of Definition 3.10.*

Proof. It is directed by reasoning's of Theorems 3.4-3.7. ∎

The next result confirms how well the recommended divergence measures $\bar{D}_1$ and $\bar{D}_2$ perform in comparison to the strict inclusion relation.

Theorem 3.12. *Let A_1, A_2 and A_3 be three FFSs on U. If $A_1 \subseteq A_2 \subseteq A_3$ with $\mu_{A_1} \leq \mu_{A_2} \leq \mu_{A_3}$ and $\nu_{A_1} > \nu_{A_2} > \nu_{A_3}$ or $\mu_{A_1} < \mu_{A_2} < \mu_{A_3}$ and $\nu_{A_1} \geq \nu_{A_2} \geq \nu_{A_3}$, or $\mu_{A_1} < \mu_{A_2} < \mu_{A_3}$ and $\nu_{A_1} > \nu_{A_2} > \nu_{A_3}$. Then $\bar{D}_1$ and $\bar{D}_2$ satisfies*

$$\bar{D}_k(A_1, A_3) > \max\{\bar{D}_k(A_1, A_2), \bar{D}_k(A_2, A_3)\}.$$

Proof. It is directed by reasoning's of Theorems 3.4-3.7. ∎

4. Transformation of Real Data into Fermatean Fuzzy Data

The motivations behind the extensions of fuzzy set theory are to provide the mechanism to deal with the uncertainty occurred in real-life problems. Due to it, the fuzzification of the real data is of paramount importance. There exist many techniques to fuzzify the data. But there does not exist a technique for obtaining the data in Fermatean fuzzy form. Thus we provide a new technique to transform the data into Fermatean fuzzy form. Before going into the main discussion, let L^* denote the set of all ordered pairs such that $L^* = \{(M, N) \mid (M, N) \in [0, 1] \times [0, 1] \ \& \ M + N \leq 1\}$.

Definition 4.1. The mapping $F : [0, 1]^3 \to L^*$ given by

$$F(\mu, c, t) = (M(\mu, c, t), N(\mu, c, t)),$$

where

$$M(\mu, c, t) = ((1 - tc)\mu)^{\frac{1}{3}},$$
$$N(\mu, c, t) = (1 - (1 - tc)\mu - tc)^{\frac{1}{3}},$$

satisfies that

1. If $c_1 > c_2$, then $\pi(F(\mu, c_1, t)) > \pi(F(\mu, c_2, t))$.
2. If $t_1 > t_2$, then $M(\mu, c, t_1) < M(\mu, c, t_2)$ and $N(\mu, c, t_1) < N(\mu, c, t_2)$, for all $\mu, c \in [0, 1]$.
3. $F(0, c, t) = \left(0, (1 - tc)^{\frac{1}{3}}\right)$, for all $c, t \in [0, 1]$.
4. $F(\mu, 0, t) = \left(\mu^{\frac{1}{3}}, (1 - \mu)^{\frac{1}{3}}\right)$, for all $\mu, t \in [0, 1]$.

5. $F(\mu, c, 0) = \left(\mu^{\frac{1}{3}}, (1-\mu)^{\frac{1}{3}}\right)$, for all $\mu, c \in [0,1]$.

6. $\pi\left(F(\mu, c, t)\right) = (tc)^{\frac{1}{3}}$.

Theorem 4.2. *Let $B = \{\ (\mu(y))\ \mid\ y \in Y\ \}$ is the real data (or in the form of fuzzy set) and let $\pi, t : Y \to [0,1]$ be two mappings. Then*

$$\begin{aligned} A &= \{F\left(\mu(y), \pi(y), t(y)\right) \mid y \in Y\} \\ &= \{(M(\mu(y), \pi(y), t(y)), N(\mu(y), \pi(y), t(y))) \mid y \in Y\} \\ &= \left\{\left(\left((1-t(y)\pi(y))\mu(y)\right)^{\frac{1}{3}}, \left(1-(1-t(y)\pi(y))\mu(y) - t(y)\pi(y)\right)^{\frac{1}{3}}\right) \mid y \in Y\right\} \end{aligned} \tag{4.1}$$

is a Fermatean fuzzy set.

To show A is a FFS, we need to prove that $(M(\mu(y), c(y), t(y)))^3 + (N(\mu(y), c(y), t(y)))^3 \leq 1$ or $(M(\mu(y), c(y), t(y)))^3 + (N(\mu(y), c(y), t(y)))^3 + \pi^3(y) = 1$. For simplifications, we write μ, c, and t instead of $\mu(y), c(y)$, and $t(y)$. From (4.1), we have

$$\begin{aligned} (M(\mu, c, t))^3 + (N(\mu, c, t))^3 &= \left(\left((1-tc)\mu\right)^{\frac{1}{3}}\right)^3 + \left(\left(1-(1-tc)\mu - tc\right)^{\frac{1}{3}}\right)^3 \\ &= (1-tc)\mu + 1 - (1-tc)\mu - tc \\ &= 1 - tc \\ &\leq 1. \end{aligned}$$

Remark 4.3. It is important to note that the parameter t in Definition 4.1 work as a control parameter which control the values of membership and non-MDs. For lesser values of t, we obtain higher values for the MDs and non-MDs.

Remark 4.4. We are motivated from Jurio et al. [12] work of transferring the fuzzy data into Intuitionistic fuzzy data. He used different parameters to construct Intuitionistic fuzzy sets (IFSs). But his proposed technique does not work for FFSs. Thus we have proposed a refined technique to construct FFSs from real or fuzzy data. Also, we control the values of MDs and non-MDs by controlling the values of the parameter t.

Example 4.5. Let $U = \{u_1, u_2, u_3\}$ be the set of universe and let $B = \{(u_1, 0.5), (u_2, 0.2), (u_3, 0.8)\}$. We fix parameters c and t as 0.2 and 0.3, respectively. The resultant FFS is obtained which is

$$A = \{(u_1, 0.7775, 0.7775), (u_2, 0.5729, 0.9094), (u_3, 0.9094, 0.5729)\}.$$

We change the values of the parameter t over its range and further observe the behavior of membership and non-membership values. We represent the resultant FFS correspond to t as A_t, that is, A_0 for $t = 0$ and so on.

$$\begin{aligned} A_0 &= \{(u_1, 0.7937, 0.7937), (u_2, 0.5848, 0.9283), (u_3, 0.9283, 0.5848)\} \\ A_{0.2} &= \{(u_1, 0.7830, 0.7830), (u_2, 0.5769, 0.9158), (u_3, 0.9158, 0.5769)\} \\ A_{0.4} &= \{(u_1, 0.7719, 0.7719), (u_2, 0.5688, 0.9029), (u_3, 0.9029, 0.5688)\} \\ A_{0.6} &= \{(u_1, 0.7606, 0.7606), (u_2, 0.5604, 0.8896), (u_3, 0.8896, 0.5604)\} \\ A_{0.8} &= \{(u_1, 0.7489, 0.7489), (u_2, 0.5518, 0.8759), (u_3, 0.8759, 0.5518)\} \\ A_1 &= \{(u_1, 0.7368, 0.7368), (u_2, 0.5429, 0.8618), (u_3, 0.8618, 0.5429)\} \end{aligned}$$

Using this data, we draw MDs and non-MDs in Figures 3 and 4, respectively. Figure 3 consist of six lines and each line connecting three points. The six lines draw against the membership values of A_0, $A_{0.2}$, $A_{0.4}$, $A_{0.6}$, $A_{0.8}$, and A_1. The lowest line in the graph generated against A_1 and upper one against A_0. Figure 3 provides the graphical verification that the variations in the values of parameter t result different MDs. Similarly, we observe the behavior of non-MDs in Figures 4, where the lowest and highest lines generated against A_1 and A_0, respectively.

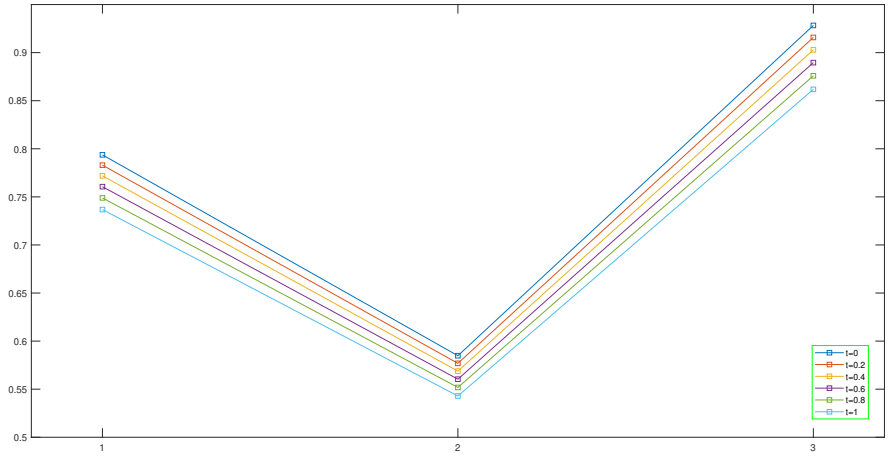

Fig. 3. Change in membership values for different values of t

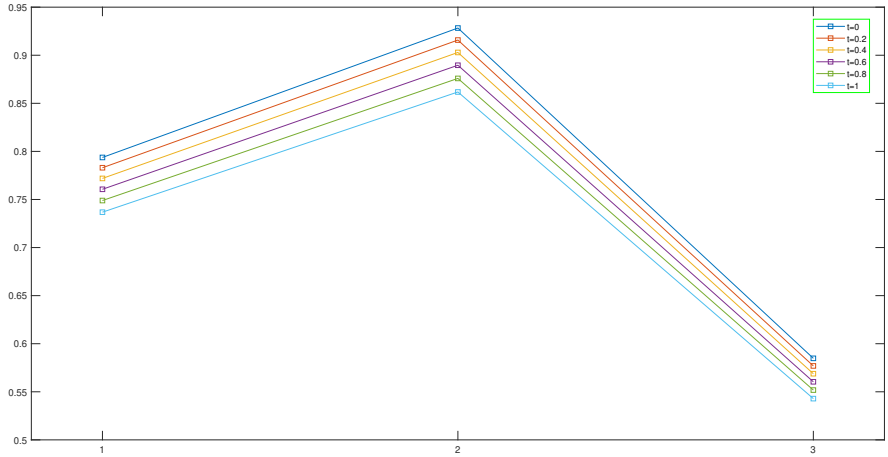

Fig. 4. Change in non-membership values for different values of t

5. Applications

The applications of the suggested divergence measures are included in this section. There are two subsections in it: In Section 5.1, the VIKOR strategy for FFSs is expanded. The ranking of small cars subjected to ANCAP safety testing from 2019 to 2021 is presented in Section 5.2.

5.1. Fermatean Fuzzy VIKOR Method

In this section, the VIKOR approach is expanded to include FFSs. This approach is created using the suggested divergence measurements. It accepts input in the form of FFS and linguistic variables.

1. The list of options is evaluated by the experts $E_k, k = \{1, 2, \dots, \ell\}$ using the suggested criteria. To depict the assessments, they can either directly input FFSs or use language variables. Fermatean fuzzy (FF) data are created from the linguistic matrix data. Thus, we get ℓ FF matrices $\left(M^k = \left[\chi_{ij}^k\right] = \left[\left(\mu_{ij}^k, \nu_{ij}^k\right)\right], k \in \{1, 2, \dots, \ell\}\right)$ from ℓ decision makers.

2. Any aggregation operator specified in [25] can be used to aggregate the data in the FF matrices.

3. The weight of the criterion varies in MCDM problems that are encountered in real life. For this reason, the weight vector $\omega = \{\omega_1, \omega_2, \dots, \omega_n\}$ is affixed to the list of requirements, where $0 \leq \omega_j \leq 1$ and $\sum_{j=1}^{n} \omega_j = 1$. Using divergence metrics on a combined FF matrix, we can construct the weight vector as follows:

$$\omega_j = \frac{\frac{1}{m-1}\left(\sum_{i=1}^{m}\sum_{k=1}^{m} \bar{D}_k\left(\chi_{ij}, \chi_{kj}\right)\right)}{\sum_{j=1}^{n}\left[\frac{1}{m-1}\left(\sum_{i=1}^{m}\sum_{k=1}^{m} \bar{D}_k\left(\chi_{ij}, \chi_{kj}\right)\right)\right]}, \quad j = 1, 2, \dots, n. \tag{5.1}$$

4. Calculate the positive ideal (PI) and negative ideal (NI) FFVs for each attribute. These characteristics direct us toward the best option and away from the least desirable one. The PI and NI FFVs are discovered using Equations (5.2) and (5.3), respectively.

$$PI_j = \left\{\left(\max_{i=1}^{m}(\mu_{ij}), \min_{i=1}^{m}(\nu_{ij})\right)\right\}, \tag{5.2}$$

$$NI_j = \left\{\left(\min_{i=1}^{m}(\mu_{ij}), \max_{i=1}^{m}(\nu_{ij})\right)\right\}, \quad j = 1, 2, \dots, n. \tag{5.3}$$

5. Using $\bar{D}_1$ and $\bar{D}_2$, the divergence between each FFV and PI FFV, as well as PI and NI FFVs, is estimated.

6. Equations (5.4), (5.5), and (5.6), respectively, construct the group utility index $\bar{S}$,

individual regret index $\bar{R}$, and compromise index $\bar{Q}$, where

$$\bar{S}(u_i) = \sum_{j=1}^{n} \omega_j \cdot \frac{\bar{D}_k(PI_j, \chi_{ij})}{\bar{D}_k(PI_j, NI_j)}, \tag{5.4}$$

$$\bar{R}(u_i) = \max_{j=1}^{n} \omega_j \cdot \frac{\bar{D}_k(PI_j, \chi_{ij})}{\bar{D}_k(PI_j, NI_j)}, \tag{5.5}$$

$$\bar{Q}(u_i) = \lambda \cdot \frac{\bar{S}(u_i) - \min\limits_{i'=1}^{m} \bar{S}(u_{i'})}{\max\limits_{i'=1}^{m} \bar{S}(u_{i'}) - \min\limits_{i'=1}^{m} \bar{S}(u_{i'})} + (1-\lambda) \cdot \frac{\bar{R}(u_i) - \min\limits_{i'=1}^{m} \bar{R}(u_{i'})}{\max\limits_{i'=1}^{m} \bar{R}(u_{i'}) - \min_{i'=1}^{m} \bar{R}(u_{i'})}, \tag{5.6}$$

where χ_{ij} is the FFV for i^{th} alternative against j^{th} criterion.

7. By placing $\bar{S}$, $\bar{R}$, and $\bar{Q}$ in increasing order, three ranking lists are created. If the following two conditions hold true, the option u_i associated with the smallest value ($u^1 = \min_{i=1}^{m} \bar{Q}(u_i)$) of $\bar{Q}$ is ranked best (compromise solution):

   C1. The ideal option found with "acceptable advantage" if

   $$u^2 - u^1 \geq \frac{1}{m-1},$$

   where u^2 is the next-to-last minimum in the $\bar{Q}$ list.

   C2. If the best option appears on both the $\bar{S}$ and $\bar{R}$ lists, it is come with "acceptable stability" (that is, minimum in both lists).

   If one of the aforementioned requirements is violated, a collection of compromise solutions is procured.

   - If C2 violates, the compromise solution is composed of the equivalent u^1 and u^2 options.
   - A compromise solution set has L members as a result of the C1 violation, where L is the maximum for which

   $$u^L - u^1 < \frac{1}{m-1}.$$

5.2. Selection of Small Car Based on ANCAP Safety Ratings

The application of the suggested method is provided in this section. The information was obtained from the ANCAP's official website. ANCAP is an independent automotive safety organization with a base in Australasia that was founded in 1993 and has rated the safety of tens of thousands of new vehicle makes models and variants. It offers comparisons of the relative levels of safety of various-sized automobiles. In the case of a collision, ANCAP safety ratings offer protection for passengers and pedestrians as well as the vehicle's technological capacity to prevent or lessen the impacts of a collision.

On there official website, we have searched the data with the following parameters: Category: Small cars, Safety Ratings (All), Ratings years 2019-21, and Fuel type: Conventional. The thirteen vehicles lie in the above mentioned search, that is, we obtained the data of 13

small cars tested from 2019 to 2021 and their fuel type is conventional. It includes the Citroen C4, Audi A3, SEAT Leon, Cupra Leon, Kia Cerato (S & sport variant), Kia Cerato, BMW 2 Series Gran Coupé, Volkswagen Golf, Skoda Scala, BMW 1 Series, Ford Focus, Mercedes-Benz B-Class, and Mazda 3. All of the small cars included in the search has five stars safety rating except Kia Cerato (S & sport variant). Kia Cerato (S & sport variant) has four star safety ratings. Their rating is based on the set of following criteria: Adult Occupant Protection, Child Occupant Protection, Vulnerable Road User Protection and Safety Assist. The details about the each criterion is provided in Figure 5. We have collected the data of thirteen small cars from their official website.

The available data is in the form of percentage, we have converted it into decimal form and present in Table 1. We have transformed the real data of Table 1 into FF data using the method discussed in Section 4. We have taken the values of parameters c and t equal to 0.2 and 1, respectively. The obtained FFS is displayed in Table 2.

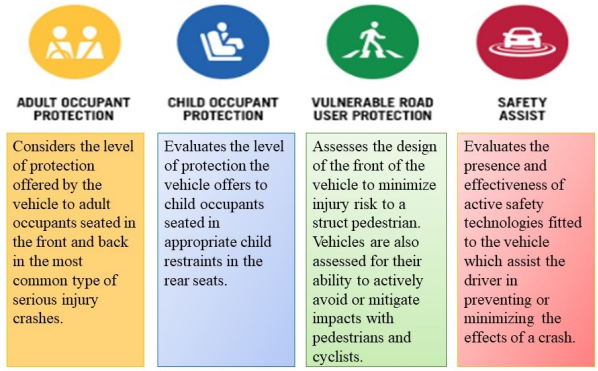

Fig. 5. Criteria explanations

Table 1. ANCAP Safety Ratings

Model	Adult OP	Child OP	VRUP	Safety Assist
Citroen C4 (u_1)	0.76	0.81	0.57	0.62
Audi A3 (u_2)	0.89	0.81	0.68	0.73
SEAT Leon (u_3)	0.92	0.88	0.71	0.80
Cupra Leon (u_4)	0.91	0.88	0.71	0.80
Kia Cerato (S & sport variant) (u_5)	0.90	0.83	0.55	0.71
Kia Cerato (u_6)	0.90	0.83	0.72	0.73
BMW 2 Series Gran Coupé (u_7)	0.94	0.89	0.76	0.73
Volkswagen Golf (u_8)	0.95	0.89	0.76	0.80
Skoda Scala (u_9)	0.97	0.87	0.81	0.76
BMW 1 Series (u_{10})	0.83	0.89	0.76	0.73
Ford Focus (u_{11})	0.96	0.87	0.72	0.72
Mercedes-Benz B-Class (u_{12})	0.96	0.92	0.78	0.77
Mazda 3 (u_{13})	0.98	0.89	0.81	0.76

OP = Occupant Protection, VRUP = Vulnerable road user protection

Table 2. ANCAP Safety Ratings in FFSs for parameters $c = 0.2$

Model	Adult OP	Child OP	VRUP	Safety Assist
u_1	$(0.8472, 0.5769)$	$(0.8653, 0.5337)$	$(0.7697, 0.7007)$	$(0.7916, 0.6724)$
u_2	$(0.8929, 0.4448)$	$(0.8653, 0.5337)$	$(0.8163, 0.6350)$	$(0.8359, 0.6000)$
u_3	$(0.9029, 0.4000)$	$(0.8896, 0.4579)$	$(0.8282, 0.6145)$	$(0.8618, 0.5429)$
u_4	$(0.8996, 0.4160)$	$(0.8896, 0.4579)$	$(0.8282, 0.6145)$	$(0.8618, 0.5429)$
u_5	$(0.8963, 0.4309)$	$(0.8724, 0.5143)$	$(0.7606, 0.7114)$	$(0.8282, 0.6145)$
u_6	$(0.8963, 0.4309)$	$(0.8724, 0.5143)$	$(0.8320, 0.6073)$	$(0.8359, 0.6000)$
u_7	$(0.9094, 0.3634)$	$(0.8929, 0.4448)$	$(0.8472, 0.5769)$	$(0.8359, 0.6000)$
u_8	$(0.9126, 0.3420)$	$(0.8929, 0.4448)$	$(0.8472, 0.5769)$	$(0.8618, 0.5429)$
u_9	$(0.9189, 0.2884)$	$(0.8862, 0.4703)$	$(0.8653, 0.5337)$	$(0.8472, 0.5769)$
u_{10}	$(0.8724, 0.5143)$	$(0.8929, 0.4448)$	$(0.8472, 0.5769)$	$(0.8359, 0.6000)$
u_{11}	$(0.9158, 0.3175)$	$(0.8862, 0.4703)$	$(0.8320, 0.6073)$	$(0.8320, 0.6073)$
u_{12}	$(0.9158, 0.3175)$	$(0.9029, 0.4000)$	$(0.8545, 0.5604)$	$(0.8509, 0.5688)$
u_{13}	$(0.9221, 0.2520)$	$(0.8929, 0.4448)$	$(0.8653, 0.5337)$	$(0.8472, 0.5769)$

OP = Occupant Protection, VRUP = Vulnerable road user protection

Next, we apply the proposed VIKOR method to the FF data. The details steps of VIKOR method for FF data are explained in Section 5.1. We have acquire the FF data or FF matrix, therefore, we start the process from Step 3. $\omega = \{\omega_1 = 0.2, \omega_2 = 0.3, \omega_3 = 0.25, \omega_4 = 0.25\}$ is taken as weight vector to distinguish the importance of criteria. The interested candidate alter the weight vector according to his need and experience. Also, there are different subjective and objective methods to get the criteria weights. It's depend on the person who want the ranking of small cars. He can choose any method to assign the criteria weights.

In the next step (Step 4), the PI and NI FFVs are determined by Equations (5.2) and (5.3). We employ these equations on Table 2 to get PI and NI FFVs.

$$\begin{aligned} PI = \{&PI_1 = (0.9221, 0.2520), PI_2 = (0.9029, 0.4000), PI_3 = (0.8653, 0.5337), \\ &PI_4 = (0.8618, 0.5429)\} \\ NI = \{&NI_1 = (0.8472, 0.5769), NI_2 = (0.8653, 0.5337), NI_3 = (0.7606, 0.7114), \\ &NI_4 = (0.7916, 0.6724)\}. \end{aligned}$$

In Step 5, the divergence between each FFV (Table 2) and PI FFV is calculated by the measure $\bar{D}_2$ presented in (3.8). Also, the divergence between PI and NI FFVs are calculated. We have taken $\lambda = 0.1$ and $\beta = 2$ for $\bar{D}_2$ in (3.8). The results are presented in matrix

$D = [d_{ij}]_{13\times 4}$, (5.7), where $d_{ij} = \bar{D}_2(PI_j, \chi_{ij})$.

$$D = \begin{bmatrix} 0.6221 & 0.2690 & 0.3439 & 0.2649 \\ 0.4021 & 0.2690 & 0.2046 & 0.1150 \\ 0.3182 & 0.1197 & 0.1627 & 0 \\ 0.3489 & 0.1197 & 0.1627 & 0 \\ 0.3767 & 0.2314 & 0.3677 & 0.1444 \\ 0.3767 & 0.2314 & 0.1482 & 0.1150 \\ 0.2451 & 0.0931 & 0.0868 & 0.1150 \\ 0.2004 & 0.0931 & 0.0868 & 0 \\ 0.0831 & 0.1446 & 0 & 0.0684 \\ 0.5217 & 0.0931 & 0.0868 & 0.1150 \\ 0.1476 & 0.1446 & 0.1482 & 0.1299 \\ 0.1476 & 0 & 0.0536 & 0.0520 \\ 0 & 0.0931 & 0 & 0.0684 \end{bmatrix} \tag{5.7}$$

The divergence measures between PI and NI FFVs are presented in (5.8).

$$E = [0.6221 \quad 0.2690 \quad 0.3677 \quad 0.2649] \tag{5.8}$$

Matrix F in (5.9) is obtained by dividing the Matrix D by E and then multiplying with weight vector, that is, $F = \omega \times \frac{D}{E} = \omega \times \frac{\bar{D}_2(PI_j, \chi_{ij})}{\bar{D}_2(PI_j, NI_j)}$.

$$F = \begin{bmatrix} 0.2000 & 0.3000 & 0.2338 & 0.2500 \\ 0.1293 & 0.3000 & 0.1391 & 0.1086 \\ 0.1023 & 0.1335 & 0.1106 & 0 \\ 0.1122 & 0.1335 & 0.1106 & 0 \\ 0.1211 & 0.2581 & 0.2500 & 0.1363 \\ 0.1211 & 0.2581 & 0.1008 & 0.1086 \\ 0.0788 & 0.1038 & 0.0590 & 0.1086 \\ 0.0644 & 0.1038 & 0.0590 & 0 \\ 0.0267 & 0.1613 & 0 & 0.0645 \\ 0.1677 & 0.1038 & 0.0590 & 0.1086 \\ 0.0475 & 0.1613 & 0.1008 & 0.1226 \\ 0.0475 & 0 & 0.0365 & 0.0491 \\ 0 & 0.1038 & 0 & 0.0645 \end{bmatrix} \tag{5.9}$$

In Step 6, the $\bar{S}$, $\bar{R}$, and $\bar{Q}$ are calculated by (5.4), (5.5), and (5.6), respectively.

$$\begin{array}{c} \\ \bar{S} \\ \bar{R} \\ \bar{Q} \\ \\ \bar{S} \\ \bar{R} \\ \bar{Q} \end{array} \begin{array}{c} \begin{array}{ccccccc} u_1 & u_2 & u_3 & u_4 & u_5 & u_6 & u_7 \end{array} \\ \begin{bmatrix} 0.984 & 0.677 & 0.346 & 0.356 & 0.766 & 0.589 & 0.350 \\ 0.300 & 0.300 & 0.134 & 0.134 & 0.258 & 0.258 & 0.109 \\ 1.000 & 0.820 & 0.294 & 0.299 & 0.788 & 0.684 & 0.246 \end{bmatrix} \\ \begin{array}{cccccc} u_8 & u_9 & u_{10} & u_{11} & u_{12} & u_{13} \end{array} \\ \begin{bmatrix} 0.227 & 0.253 & 0.439 & 0.432 & 0.133 & 0.168 \\ 0.104 & 0.161 & 0.168 & 0.161 & 0.049 & 0.104 \\ 0.164 & 0.294 & 0.416 & 0.399 & 0 & 0.130 \end{bmatrix} \end{array} \tag{5.10}$$

In Step 7, three ranking arrangements are acquired by classifying $\bar{S}$, $\bar{R}$, and $\bar{Q}$ from (5.10). Preference given to the minimum values of $\bar{S}$, $\bar{R}$, and $\bar{Q}$. $\bar{S}$, $\bar{R}$, and $\bar{Q}$ has minimum values for the alternative u_{12} (Mercedes-Benz B-Class). It ensures that the small car Mercedes-Benz B-Class acquired with acceptable stability. Also, by sorting $\bar{Q}$, the last two minimum values are $\bar{Q}(u_{12}) = 0$ and $\bar{Q}(u_{13}) = 0.130$. Since $\bar{Q}(u_{13}) - \bar{Q}(u_{12}) = 0.130 - 0 = 0.130 > \frac{1}{m-1} = \frac{1}{13-1} = 0.0833$, that is, acceptable advantage achieved. Thus, the optimum alternative u_{12} acquire with acceptable stability and acceptable advantage.

$$\begin{matrix}\bar{S}\\ \bar{R}\\ \bar{Q}\end{matrix}\begin{bmatrix} u_{12} \succ u_{13} \succ u_8 \succ u_9 \succ u_3 \succ u_7 \succ u_4 \succ u_{11} \succ u_{10} \succ u_6 \succ u_2 \succ u_5 \succ u_1 \\ u_{12} \succ u_{13} \succ u_8 \succ u_7 \succ u_3 \succ u_4 \succ u_9 \succ u_{11} \succ u_{10} \succ u_6 \succ u_5 \succ u_2 \succ u_1 \\ u_{12} \succ u_{13} \succ u_8 \succ u_7 \succ u_3 \succ u_9 \succ u_4 \succ u_{11} \succ u_{10} \succ u_6 \succ u_5 \succ u_2 \succ u_1 \end{bmatrix} \tag{5.11}$$

The final ranking of the small cars based on ANCAP Safety Ratings is obtained from (5.11) and given as

$$u_{12} \succ u_{13} \succ u_8 \succ u_7 \succ u_3 \succ u_9 \succ u_4 \succ u_{11} \succ u_{10} \succ u_6 \succ u_5 \succ u_2 \succ u_1.$$

Remark 5.1. It is important to note that by changing the value of the parameter t to transform the data into FF data does not effect the ranking of small cars. Please kept in mind, we are using $\bar{D}_2$ to calculate divergence measures. Also, the different values of β and δ in (3.8) do not alter the ranking of small cars.

Remark 5.2. We have solved the problem discussed in Section 5.2 by the divergence measure $\bar{D}_1$ defined in (3.1). After calculations, we obtain the small car u_{12} with acceptable stability, but lack the acceptable advantage. Thus, the set of compromise solution is obtained and written as

$$\{u_{12} \succ u_{13} \succ u_8\} \succ u_7 \succ u_3 \succ u_4 \succ u_9 \succ u_{11} \succ u_{10} \succ u_6 \succ u_5 \succ u_2 \succ u_1.$$

6. Comparison

In this section, we compare the suggested MCDM method with the MCDM techniques that have already been published. We choose the FF environment for comparison and the comparison details are shown in Table 3. It shows the author's details, their proposed methods, and rankings. We have seen small changes in the rankings of small cars using different methods in Table 3. The abbreviations used in Table 3 come from the cited papers.

6.1. Comparison in pattern recognition problems

The classification of an unfamiliar pattern into some recognized patterns is known as pattern recognition. When working in a fuzzy environment, compatibility measurements like divergence, distance, correlation, similarity, accuracy, etc. are used to accomplish pattern recognition. Here, for pattern identification, we use some of the existing distance measures with the suggested divergence measures. Senapati and Yager [27] extended Euclidean distance ($\bar{D}_3$), and Deng and Wang [6] proposed Hellinger ($\bar{D}_4$) and triangular ($\bar{D}_5$) distances for FFSs.

Table 3. Comparison with existing MCDMs Methods

Authors & Methods	Rankings
Senapati & Yager [25] FFWA operator	$u_{13} \succ u_{12} \succ u_9 \succ u_8 \succ u_7 \succ u_3 \succ u_4 \succ u_{11} \succ u_{10} \succ u_6 \succ u_2 \succ u_5 \succ u_1$
Senapati & Yager [25] FFWG operator	$u_{13} \succ u_{12} \succ u_9 \succ u_8 \succ u_7 \succ u_{11} \succ u_3 \succ u_4 \succ u_{10} \succ u_6 \succ u_2 \succ u_5 \succ u_1$
Senapati & Yager [25] FFWPA operator	$u_{13} \succ u_{12} \succ u_9 \succ u_8 \succ u_7 \succ u_3 \succ u_4 \succ u_{11} \succ u_{10} \succ u_6 \succ u_2 \succ u_5 \succ u_1$
Senapati & Yager [25] FFWPG operator	$u_{13} \succ u_{12} \succ u_9 \succ u_8 \succ u_7 \succ u_3 \succ u_4 \succ u_{11} \succ u_{10} \succ u_6 \succ u_2 \succ u_5 \succ u_1$
Akram et al. [7] FFYWA operator	$u_{13} \succ u_{12} \succ u_9 \succ u_8 \succ u_7 \succ u_3 \succ u_4 \succ u_{11} \succ u_{10} \succ u_6 \succ u_2 \succ u_5 \succ u_1$
Akram et al. [7] FFYOWA operator	$u_{13} \succ u_{12} \succ u_9 \succ u_8 \succ u_7 \succ u_3 \succ u_4 \succ u_{11} \succ u_{10} \succ u_6 \succ u_2 \succ u_5 \succ u_1$
Akram et al. [7] FFYWG operator	$u_{12} \succ u_{13} \succ u_9 \succ u_8 \succ u_7 \succ u_3 \succ u_4 \succ u_{11} \succ u_{10} \succ u_6 \succ u_2 \succ u_5 \succ u_1$
Akram et al. [7] FFYOWG operator	$u_{12} \succ u_{13} \succ u_9 \succ u_8 \succ u_7 \succ u_3 \succ u_4 \succ u_{11} \succ u_{10} \succ u_6 \succ u_2 \succ u_5 \succ u_1$
Ghorabaee et al. [13] WASPAS method	$u_{13} \succ u_{12} \succ u_9 \succ u_8 \succ u_7 \succ u_3 \succ u_4 \succ u_{11} \succ u_{10} \succ u_6 \succ u_2 \succ u_5 \succ u_1$
Akram et al. [1] FFEWA operator	$u_{13} \succ u_{12} \succ u_9 \succ u_8 \succ u_7 \succ u_{11} \succ u_3 \succ u_4 \succ u_{10} \succ u_6 \succ u_2 \succ u_5 \succ u_1$
Akram et al. [1] FFEOWA operator	$u_{12} \succ u_{13} \succ u_9 \succ u_8 \succ u_7 \succ u_3 \succ u_4 \succ u_{11} \succ u_{10} \succ u_6 \succ u_2 \succ u_5 \succ u_1$
Akram et al. [1] GFFEWA operator	$u_{13} \succ u_{12} \succ u_9 \succ u_8 \succ u_7 \succ u_{11} \succ u_3 \succ u_4 \succ u_{10} \succ u_6 \succ u_2 \succ u_5 \succ u_1$
Akram et al. [1] GFFEOWA operator	$u_{12} \succ u_{13} \succ u_9 \succ u_8 \succ u_7 \succ u_3 \succ u_4 \succ u_{11} \succ u_{10} \succ u_6 \succ u_2 \succ u_5 \succ u_1$
Gul [8] SAW method	$u_{12} \succ u_{13} \succ u_8 \succ u_7 \succ u_3 \succ u_9 \succ u_4 \succ u_{11} \succ u_{10} \succ u_6 \succ u_5 \succ u_2 \succ u_1$
Gul [8] ARAS method	$u_{13} \succ u_{12} \succ u_8 \succ u_7 \succ u_3 \succ u_4 \succ u_9 \succ u_{11} \succ u_{10} \succ u_6 \succ u_5 \succ u_2 \succ u_1$
Gul [8] VIKOR method	$u_{12} \succ u_{13} \succ u_8 \succ u_7 \succ u_3 \succ u_4 \succ u_9 \succ u_{11} \succ u_{10} \succ u_6 \succ u_5 \succ u_2 \succ u_1$
Deng & Wang [5] EFF method	$u_{12} \succ u_{13} \succ u_8 \succ u_7 \succ u_3 \succ u_9 \succ u_4 \succ u_{11} \succ u_{10} \succ u_6 \succ u_5 \succ u_2 \succ u_1$
Hadi et al. [9] FFHWA operator	$u_{13} \succ u_{12} \succ u_9 \succ u_8 \succ u_7 \succ u_{11} \succ u_3 \succ u_4 \succ u_{10} \succ u_6 \succ u_2 \succ u_5 \succ u_1$
Hadi et al. [9] FFHOWA operator	$u_{13} \succ u_{12} \succ u_9 \succ u_8 \succ u_7 \succ u_3 \succ u_4 \succ u_{11} \succ u_{10} \succ u_6 \succ u_2 \succ u_5 \succ u_1$
Hadi et al. [9] FFHHWA operator	$u_{13} \succ u_{12} \succ u_9 \succ u_8 \succ u_7 \succ u_{11} \succ u_3 \succ u_4 \succ u_{10} \succ u_6 \succ u_2 \succ u_5 \succ u_1$
Mishra et al. [18] CRITIC-EDAS method	$u_{13} \succ u_{12} \succ u_9 \succ u_8 \succ u_7 \succ u_{11} \succ u_3 \succ u_4 \succ u_{10} \succ u_6 \succ u_2 \succ u_5 \succ u_1$
Proposed VIKOR method by $\bar{D}_1$	$\{u_{12} \succ u_{13} \succ u_8\} \succ u_7 \succ u_3 \succ u_4 \succ u_9 \succ u_{11} \succ u_{10} \succ u_6 \succ u_5 \succ u_2 \succ u_1$
Proposed VIKOR method by $\bar{D}_2$	$u_{12} \succ u_{13} \succ u_8 \succ u_7 \succ u_3 \succ u_9 \succ u_4 \succ u_{11} \succ u_{10} \succ u_6 \succ u_5 \succ u_2 \succ u_1$

$$\bar{D}_3(A_1, A_2) = \sqrt{\frac{1}{2n}\sum_{i=1}^{n}\left[\left(\mu^3_{A_1}(u_i) - \mu^3_{A_2}(u_i)\right)^2 + \left(\nu^3_{A_1}(u_i) - \nu^3_{A_2}(u_i)\right)^2 + \left(\pi^3_{A_1}(u_i) - \pi^3_{A_2}(u_i)\right)^2\right]}$$

$$\bar{D}_4(A_1, A_2) = \sqrt{\frac{1}{2n}\sum_{i=1}^{n}\left[\left(\sqrt{\mu^3_{A_1}(u_i)} - \sqrt{\mu^3_{A_2}(u_i)}\right)^2 + \left(\sqrt{\nu^3_{A_1}(u_i)} - \sqrt{\nu^3_{A_2}(u_i)}\right)^2\right]}$$

$$\bar{D}_5(A_1, A_2) = \sqrt{\frac{1}{2n}\sum_{i=1}^{n}\left[\frac{\left(\mu^3_{A_1}(u_i) - \mu^3_{A_2}(u_i)\right)^2}{\mu^3_{A_1}(u_i) + \mu^3_{A_2}(u_i)} + \frac{\left(\nu^3_{A_1}(u_i) - \nu^3_{A_2}(u_i)\right)^2}{\nu^3_{A_1}(u_i) + \nu^3_{A_2}(u_i)}\right]}$$

The question arises, what will be the final decision when various measures categorize unidentified patterns into various classes? How do we choose the metrics when they yield disparate results? We will see that the divergence measure $\bar{D}_2$ is a more certain and reliable measure in this regard. The example that follows demonstrates our findings.

Example 6.1. Let Q_1, Q_2, Q_3, Q_4, and P be the five patterns given in the form of FFSs:

$$\begin{aligned}
P &= \{(u_1, 0.8, 0.3), (u_2, 0.6, 0.2), (u_3, 0.7, 0.5), (u_4, 0.6, 0.1)\},\\
Q_1 &= \{(u_1, 0.7, 0.4), (u_2, 0.5, 0.2), (u_3, 0.7, 0.3), (u_4, 0.4, 0.2)\},\\
Q_2 &= \{(u_1, 0.8, 0.2), (u_2, 0.6, 0.1), (u_3, 0.6, 0.1), (u_4, 0.6, 0.1)\},\\
Q_3 &= \{(u_1, 0.5, 0.1), (u_2, 0.4, 0.3), (u_3, 0.5, 0.2), (u_4, 0.8, 0.3)\},\\
Q_4 &= \{(u_1, 0.6, 0.4), (u_2, 0.7, 0.2), (u_3, 0.3, 0.4), (u_4, 0.6, 0.1)\}.
\end{aligned}$$

We can determine whether P and $Q_i, i = 1, \ldots, 4$ are similar. If there is a minimum divergence between P and Q_i, the pattern P belongs to Q_j. Table 4 and Figure 6 both display the calculated values of divergence between P and Q_i using the various divergence metrics. Labels $\mathbf{1}, \ldots, \mathbf{4}$ on X-axis in Figure 6 represents the FFSs Q_1 to Q_4, respectively.

Now, according to Table 4, P is nearest to Q_1 from the views of $\bar{D}_1$ and $\bar{D}_4$, but P is closest to Q_2 from the perspectives of $\bar{D}_2$, $\bar{D}_3$, and $\bar{D}_5$. So what will be our final decision? Also from Figure 6, the graph of divergence between P and Q_1 remains below for measures $\bar{D}_1$ and $\bar{D}_4$, and the minimum value of divergence is attained between P and Q_2 by $\bar{D}_2$, $\bar{D}_3$, and $\bar{D}_5$. In order to evaluate the effectiveness of the divergence metric, Hatzimichailidis et al. [10] defined the Degree of Confidence (DoC). For a divergence metric, the higher the value of DoC, the more reliable the measure is. A divergence measure's DoC is determined as follows:

$$DoC^{i^*} = \sum_{i=1, i\neq i^*}^{n} \left|\bar{D}_k(P, Q_{i^*}) - \bar{D}_k(P, Q_i)\right|,$$

where i^* corresponds to the FFS Q_i having minimum divergence from unknown pattern P.

Thus, we have calculated the DoC for each divergence measure and written it in Table 4. It can be seen that the DoC of $\bar{D}_2$ is much higher than other measures. This guarantee that the pattern recognition by $\bar{D}_2$ is much more confident than others.

Table 4. Divergence measures calculation for Example 6.1

	(P, Q_1)	(P, Q_2)	(P, Q_3)	(P, Q_4)	Result	DoC
$\bar{D}_1$	0.0196	0.0471	0.0687	0.0275	Q_1	0.0844
$\bar{D}_2$	0.3286	0.2471	0.4749	0.3515	Q_2	**0.4139**
$\bar{D}_3$	0.1261	0.1092	0.3016	0.2329	Q_2	0.3332
$\bar{D}_4$	0.1230	0.1261	0.2245	0.1847	Q_1	0.1662
$\bar{D}_5$	0.1673	0.1443	0.2960	0.2382	Q_2	0.2685

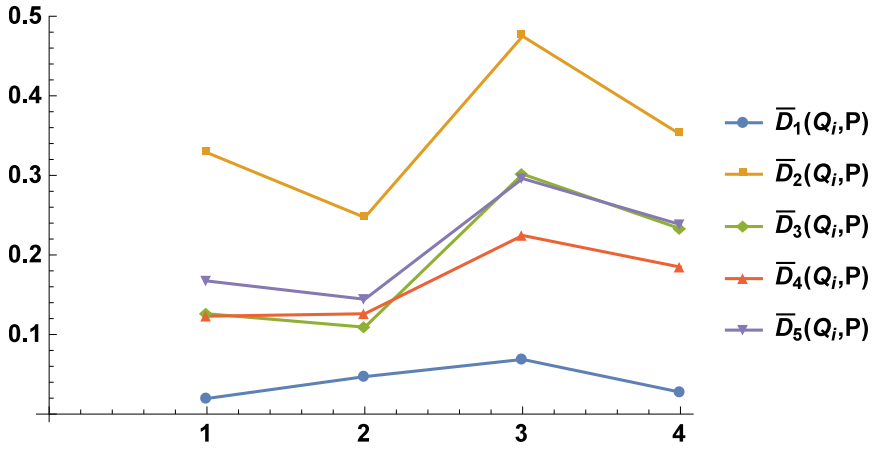

Fig. 6. Divergence between the known and unknown patterns

7. Conclusion

The study established the generalized chi-square and generalized Canberra distances-based divergence measures for FFSs. The hypotheses have been constructed to determine whether a function is a divergence measure. The proposed divergence functions' axiomatic qualities have been confirmed. Divergence measures other characteristics have been looked at to ensure their effectiveness. Additionally, research has been done on the C-IF entropy and dissimilarity metrics. Multi-criteria decision-making problems have been solved by extending and utilizing the divergence-measure-based VIKOR approach for FFSs. A method to transform the real data into FF data has been presented and justified by numerical examples. In the end, the proposed method has been employed to rank the small cars tested from 2019 to 2021 by ANCAP. ANCAP provides the safety ratings for the vehicles tested in a particular year. But it is hard for someone to choose the vehicle based on their provided rankings. Thus, the proposed MCDM method has been used to rank the thirteen small cars with conventional fuel types tested from 2019 to 2021. The suggested divergence measurements will be used in various fields, including pattern recognition, classification, and image processing. We shall define the knowledge, entropy, similarity, and dissimilarity measures for FFSs.

Acknowledgments

The authors acknowledge the financial support provided by the NSRF via the Program Management Unit for Human Resources & Institutional Development, Research and Innovation [grant number B39G660025]. Moreover, this research was supported by The Science, Research and Innovation Promotion Funding (TSRI) (Grant No. FRB660012/0168). This research block grants was managed under Rajamangala University of Technology Thanyaburi (FRB66E0648P.1).

References

[1] M. Akram, G. Shahzadi and A.A.H. Ahmadini, Decision-making framework for an effective sanitizer to reduce COVID-19 under Fermatean fuzzy environment, Journal of Mathematics, 2020 (2020), Article ID 3263407.

[2] K.T. Atanassov, Intuitionistic fuzzy sets, Fuzzy Sets Syst, 20 (1986), 87–96.

[3] S.B. Aydemir and S. Yilmaz Gunduz, Fermatean fuzzy TOPSIS method with dombi aggregation operators and its application in multi-criteria decision making, J. Intell. Fuzzy Syst., 39 (1) (2020), 851–869.

[4] D. Bhandari, N.R. Pal and D. Dutta Majumder, Fuzzy divergence, probability measure of fuzzy events and image thresholding, Pattern Recognit Lett., 13 (1992), 857–867.

[5] Z. Deng and J. Wang, Evidential Fermatean fuzzy multicriteria decision-making based on Fermatean fuzzy entropy, Int. J. Intell. Syst., 36 (10) (2021), 5866–5886.

[6] Z. Deng and J. Wang, New distance measure for Fermatean fuzzy sets and its application, Int. J. Intell. Syst., 37 (3) (2022), 1903–1930.

[7] H. Garg, G. Shahzadi and M. Akram, Decision-making analysis based on Fermatean fuzzy Yager aggregation operators with application in COVID-19 testing facility, Math. Probl. Eng., 2020 (2020), Article ID: 7279027.

[8] S. Gul, Fermatean fuzzy set extensions of SAW, ARAS, and VIKOR with applications in COVID-19 testing laboratory selection problem, Expert Syst., 38 (8) (2021), p. e12769.

[9] A. Hadi, W. Khan and A. Khan, A novel approach to MADM problems using Fermatean fuzzy Hamacher aggregation operators, Int. J. Intell. Syst., 36 (7) (2021), 3464–3499.

[10] A.G. Hatzimichailidis, G.A. Papakostas and V.G. Kaburlasos, A novel distance measure of intuitionistic fuzzy sets and its application to pattern recognition problems, Int. J. Intell. Syst., 27 (4) (2012), 396–409.

[11] S. Jeevaraj, Ordering of interval-valued Fermatean fuzzy sets and its applications, Expert Syst. Appl., 185 (2021), p.115613.

[12] A. Jurio, D. Paternain, H. Bustince, C. Guerra and G. Beliakov, A construction method of Atanassov's intuitionistic fuzzy sets for image processing, In: 2010 5th IEEE International Conference Intelligent Systems, 2010, 337–342.

[13] M. Keshavarz-Ghorabaee, M. Amiri, M. Hashemi-Tabatabaei, E.K. Zavadskas and A. Kaklauskas, A new decision-making approach based on Fermatean fuzzy sets and WASPAS for green construction supplier evaluation, Mathematics, 8 (12) (2020).

[14] M.J. Khan, J.C.R. Alcantud, P. Kumam, W. Kumam and A.N. Al-Kenani, An axiomatically supported divergence measures for q-rung orthopair fuzzy sets, Int. J. Intell. Syst., 36 (10) (2021), 6133–6155.

[15] M.J. Khan, J.C. Alcantud, P. Kumam, W. Kumam and A.N. Al-Kenani, Intuitionistic fuzzy divergences: critical analysis and an application in figure skating, Neural Comput. Appl., 34 (2022), 9123–9146.

[16] M.J. Khan, P. Kumam and W. Kumam, Theoretical justifications for the empirically successful VIKOR approach to multi-criteria decision making, Soft Comput., 25 (2021), 7761–7767.

[17] D. Liu, Y. Liu and X. Chen, Fermatean fuzzy linguistic set and its application in multicriteria decision making, Int. J. Intell. Syst., 34 (5) (2019), 878–894.

[18] A.R. Mishra, P. Rani and K. Pandey, Fermatean fuzzy CRITIC-EDAS approach for the selection of sustainable third-party reverse logistics providers using improved generalized score function, J. Ambient Intell. Humaniz. Comput., 13 (2022), 295-–311.

[19] S. Montes, I. Couso, P. Gil and C. Bertoluzza, Divergence measure between fuzzy sets, Int. J. Approx. Reason., 30 (2) (2002), 91–105.

[20] I. Montes, N.R. Pal, V. Janis and S. Montes, Divergence measures for intuitionistic fuzzy sets, IEEE Trans. Fuzzy Syst., 23 (2) (2014), 444–456.

[21] P. Rani and A.R. Mishra, Fermatean fuzzy Einstein aggregation operators-based MULTIMOORA method for electric vehicle charging station selection, Expert Syst. Appl., 182 (2021), p.115267.

[22] P. Rani, A.R. Mishra, K.R. Pardasani, A. Mardani, H. Liao and D. Streimikiene, A novel VIKOR approach based on entropy and divergence measures of Pythagorean fuzzy sets to evaluate renewable energy technologies in India, J. Clean. Prod., 238 (2019), p.117936.

[23] M. Riaz, A. Habib, M.J. Khan, and P. Kumam, Correlation coefficients for cubic bipolar fuzzy sets with applications to pattern recognition and clustering analysis, IEEE Access, 9 (2021), 109053–109066.

[24] L. Sahoo, A new score function based Fermatean fuzzy transportation problem, Results Control Optim., 4 (2021), p.100040.

[25] T. Senapati and R.R. Yager, Fermatean fuzzy weighted averaging/geometric operators and its application in multi-criteria decision-making methods, Eng. Appl. Artif. Intell., 85 (2019), 112–121.

[26] T. Senapati and R.R. Yager, Some new operations over Fermatean fuzzy numbers and application of Fermatean fuzzy WPM in multiple criteria decision making, Informatica, 30 (2) (2019), 391–412.

[27] T. Senapati and R.R. Yager, Fermatean fuzzy sets, J. Ambient Intell. Humaniz. Comput., 11 (2020), No. 2, 663–674.

[28] R.R. Yager, Pythagorean fuzzy subsets, In: 2013 joint IFSA world congress and NAFIPS annual meeting (IFSA/NAFIPS), 2013, 57–61, IEEE.

[29] R. Verma, Multiple attribute group decision-making based on order-α divergence and entropy measures under q-rung orthopair fuzzy environment, Int. J. Intell. Syst., 35 (4) (2020), 718–750.

[30] L.A. Zadeh, Fuzzy sets, Information Control, 8 (1965), 338–353.

[31] Q. Zhou, H. Mo and Y. Deng, A new divergence measure of pythagorean fuzzy sets based on belief function and its application in medical diagnosis, Mathematics, 8 (1) (2020), p.142.

Nonlinear Convex Analysis and Optimization:

An International Journal on Numerical, Computation and Applications

Contract

Nonlinear Convex Analysis and Optimization Research Centre
SCL802 8th floor, Fundamental Science Laboratory Building, Faculty of Science, King Mongkut's University of Technology Thonburi (KMUTT), 126 Pracha-Uthit Road, Bang Mod, Thung Khru, Bangkok, Thailand
Email: ncao.journal@gmail.com

Editorial Board Members

Rabian Wangkeeree
Naresuan University, Phitsanulok, Thailand
Email: rabianw@nu.ac.th
Sang-Eon Han
Jeonbuk National University, Jeonbuk, South Korea
Email: sehan@jbnu.ac.kr
Umar Batsari Yusuf
Hassan Usman Katsina Polytechnic, Katsina, Nigeria
Email: wutiphol@mathstat.sci.tu.ac.th
Habib ur Rehman
King Mongkut's University of Technology Thonburi (KMUTT), Bangkok, Thailand
Email: hrehman.hed@gmail.com
Auwal Bala Abubakar
Bayero University, Kano, Nigeria
Email: ababubakar.mth@buk.edu.ng
Izhar Uddin
Jamia Millia Islamia, New Delhi, India
Email: izharuddin1@jmi.ac.in
Abubakar Adamu
African University of Science and Technology, Abuja, Nigeria
Email: aadamu@aust.edu.ng